eLife

Reviewed Preprint
v1 • August 28, 2025
Not revised

Reviewed Preprint
v2 • September 3, 2026
Revised by authors

For correspondence:
felipe.cava@umu.se
bnan@tamu.edu

¶ Present address: Novo Nordisk Foundation Center for Biosustainability, Technical University of Denmark, Lyngby, Denmark

Competing interests: No competing interests declared

Reviewing editor: Bavesh D Kana, University of the Witwatersrand, South Africa

A novel mechanism for bacterial sporulation based on programmed peptidoglycan degradation

Carlos A Ramírez Carbó[1,2], Oihane Irazoki[3,¶], Srutha Venkatesan[1], Lauren JS Chen[1], Haylie A Morales[1], Assariel J Garcia Avila[1], Hoi-Ling Cheung[1], Felipe Cava[3] ✉, Beiyan Nan[1] ✉

[1]Department of Biology, Texas A&M University, College Station, United States • [2]The Genetics and Genomics Interdisciplinary Program, Texas A&M University, College Station, United States • [3]Department of Molecular Biology and Laboratory for Molecular Infection Medicine Sweden, Umeå Centre for Microbial Research, SciLifeLab, Umeå University, Umeå, Sweden

eLife Assessment

This **important** study elucidates the roles of two lytic transglycosylase (LTG) enzymes in the progression of spore formation in the research model species *Myxococcus xanthus*. Consistent with previous work indicating loss of peptidoglycan during the laboratory-induced rapid spore formation process, the new data demonstrate a similar loss of peptidoglycan during the normal, slow sporulation process. **Solid** evidence is provided for the roles of the two LTGs in spore formation and for interplay between the functions of these enzymes and peptidoglycan synthetic systems. These findings may have broader implications for understanding PG metabolism across a range of bacterial species.

https://doi.org/10.7554/eLife.108250.2.sa2

Abstract

Many bacteria form spores to endure unfavorable conditions. While *Firmicutes* generate endospores through cell division, sporulation in non-Firmicutes remains less understood. The Gram-negative bacterium *Myxococcus xanthus* undergoes sporulation through two distinct mechanisms: rapid sporulation triggered by chemical induction and slow sporulation driven by starvation, both occurring independently of cell division. Instead, these processes depend on the complete degradation of the peptidoglycan (PG) cell wall by two lytic transglycosylases (LTGs), LtgA and LtgB. Remarkably, LtgB programs the pace of PG degradation by LtgA during rapid sporulation, ensuring a controlled process that prevents abrupt PG breakdown and the formation of non-resistant pseudospores. In addition to regulation between LTGs, PG degradation is also influenced by its synthesis; cells exhibiting increased muropeptide production often circumvent sporulation. These findings not only reveal novel mechanisms of bacterial sporulation but also shed light on the regulatory network governing PG dynamics.

Introduction

Spores are metabolically dormant cells that can survive unfavorable conditions, including extremes of temperature, desiccation, and ionizing radiation (Huang & Hull, 2017, Hutchison et al., 2014). Sporulation, the process of spore development, is a strategy utilized by a wide variety of organisms, from bacteria and protozoa to fungi and plants. In addition to protective spore coats, spore resilience relies on cytosol dehydration and DNA compaction—key processes that decrease cell volume and alter cell shape (Higgins & Dworkin, 2012). Thus, morphological differentiation is a hallmark of sporulation. In bacterial spore formers, as peptidoglycan (PG) cell walls largely determine cell morphology, their sporulation requires profound PG remodeling.

PG is a rigid, mesh-like macromolecule that is composed of glycan strands of repeating units of N-acetyl glucosamine (GluNAc)-N-acetyl muramic acid (MurNAc) crosslinked by peptides (Egan et al., 2020). PG encloses the entire cytoplasmic membrane, and its rigidity provides mechanical support against osmotic stress. For this reason, PG is an essential structure for most bacteria and a major target for antibacterial treatments. Sporulation provides invaluable opportunities for understanding the dynamics of PG, which is controlled by multiple synthases and hydrolases. PG synthases include glycosyltransferases (GTases) that polymerize glycan strands and transpeptidases (TPases) that form peptide crosslinks (Egan et al., 2020). PG hydrolases, also known as autolysins, include glycosidases that break the glycan strands, and amidases and endo/carboxypeptidases that cleave the peptide crosslinks (Egan et al., 2020, Rohs & Bernhardt, 2021, van Heijenoort, 2011).

Firmicutes, including Gram-positive bacteria like *Bacilli* and *Clostridia*, produce endospores. Their morphological transition from rod-shaped vegetative cells to ovoid spores occurs through asymmetric cell division, resulting in the formation of a smaller forespore and a larger mother cell. Eventually, the forespore becomes an oval endospore after being engulfed by the mother cell (Higgins & Dworkin, 2012, McKenney & Eichenberger, 2012). A mature endospore contains two PG layers: the germ cell wall, derived from the forespore's original PG, and a thickened PG cortex deposited by the mother cell (Popham & Bernhards, 2015). While a few Gram-negative spore formers also belong to the *Firmicutes* phylum, they share conserved sporulation genes with *Bacilli* and *Clostridia*, which suggests similar sporulation mechanisms (Tocheva et al., 2011, Yutin & Galperin, 2013).

Sporulation by non-firmicutes bacteria has been largely overlooked. Myxobacteria, a group of Gram-negative, non-firmicutes spore formers, were first assigned to the phylum δ-proteobacteria, but recently reclassified into the newly established phylum *Myxococcota* (Waite et al., 2020). *Myxococcus xanthus* is a model organism of myxobacteria. Rod-shaped *M. xanthus* cells can undergo sporulation via two distinct pathways, both resulting in spherical spores (Kroos et al., 2025). First, in response to certain chemical signals, such as glycerol and dimethyl sulfoxide (DMSO), individual *M. xanthus* cells can rapidly transition into isolated spherical spores in aqueous environments within hours (Dworkin & Gibson, 1964). Second, millions of cells can aggregate on solid starvation media and develop into spore-filled fruiting bodies, a process that takes a few days to complete (O'Connor & Zusman, 1988). Both sporulation pathways are programmed, tightly controlled processes that involve over 1,000 genes (Muller et al., 2010, Munoz-Dorado et al., 2019). In contrast to endospore formation, cell division is not involved in either the *M. xanthus* sporulation mechanisms, and *M. xanthus* lacks the homologs of the sporulation genes in *Firmicutes* (Aramayo & Nan, 2022). Thus, sporulating *M. xanthus* must accomplish the rod-to-sphere transition through yet to be discovered PG remodeling mechanisms, which provide invaluable opportunities to investigate PG dynamics (Zhang et al., 2021).

Distinct from *Bacilli* and *Clostridia*, *M. xanthus* spores lack cortex PG (Bui et al., 2009, Zhang et al., 2020, Voelz & Dworkin, 1962). Rather, their resistance is derived from polysaccharide coats (Kottel et al., 1975, Perez-Burgos et al., 2020, Saidi et al., 2021, Muller et al., 2012). Sporulating cells that fail to deposit coat polysaccharides on their surfaces produce spherical pseudospores that lack resistance (Wartel et al., 2013, Zhang et al., 2020, Holkenbrink et al., 2014). In a pioneering study, Bui et al. did not detect muropeptides in glycerol-induced spores, indicating that *M. xanthus* degrades its PG during rapid sporulation (Bui et al., 2009). However, it remains unclear whether starvation-induced spores within fruiting bodies still retain PG and how *M. xanthus* orchestrates programmed morphological changes.

In this report, we used ultra-performance liquid chromatography (UPLC) to demonstrate that *M. xanthus* degrades PG in both sporulation pathways. Through mutagenesis studies, we identified LtgA and LtgB, two lytic transglycosylases (LTGs) essential for these sporulation pathways. Remarkably, LtgB regulates the pace of PG degradation by LtgA during rapid sporulation, preventing the formation of non- resistant pseudospores due to abrupt PG breakdown. This research not only uncovers novel mechanisms of sporulation in non-firmicutes but also highlights the crucial role of cross-regulation between PG hydrolases in maintaining cell integrity.

Results

PG is degraded in both spore types

To investigate if starvation-induced spores in *M. xanthus* fruiting bodies retain PG, we broke the fruiting bodies after 120 h of starvation and purified saculli from spores. For comparison, we also purified the sacculi from vegetative cells and glycerol-induced spores. The purification procedure yields only sedimentable PG, as all soluble fragments are removed during the washing steps. The resulting sacculi were then digested with muramidase, and the solubilized muropeptides were analyzed by UPLC (see Materials and Methods). The chromatograms in Figure 1 reflect the muropeptides released specifically from the sedimented sacculus fraction. The two spore types showed similar profiles of a discernible presence of muropeptides that resembled those found in vegetative cells, albeit in significantly reduced quantities (Figure 1). Importantly, the most abundant muropeptides identified in the vegetative cells, MurNAc-tetrapeptide monomer (M4) and MurNAc-tetrapeptide dimer (D44), were nearly absent in both spore types (Figure 1). Such residual muropeptides in both spore types are inadequate for forming continuous PG layers (Bui et al., 2009). This observation indicates that spore development in both pathways involves the breakdown of the vegetative PG cell wall.

Despite the overall decline in muropeptides, anhydro-muropeptides markedly increased in both spore types, comprising over 90% of the total muropeptides (Figure 1). Especially, anhydro-MurNAc-tetrapeptide trimer ($T444^{Anh}$) that was only detected in trace amounts in vegetative cells, became a prominent muropeptide in both spore types (Figure 1). Moreover, new anhydro-muropeptides, including anhydro, anhydro- MurNAc-tetrapeptide dimer ($D44^{Anh,Anh}$), anhydro, anhydro-MurNAc-tetrapeptide trimer ($T444^{Anh,Anh}$), and an anhydrodimer without a NAG ($D44^{Anh}$(-NAG)), were only present in spores (Figure 1). Because anhydro-muropeptides are the signature products of LTGs (Dik et al., 2017, Williams et al., 2018), their abundance in spores indicates that certain LTGs must play essential roles in *M. xanthus* sporulation.

M. xanthus sporulation requires two LTGs

The genome of *M. xanthus* encodes 14 putative LTGs (Aramayo & Nan, 2022, Ramirez Carbo et al., 2024). We imaged the cells of the 14 knockout mutants (Ramirez Carbo et al., 2024) after 6 h of glycerol induction and identified two mutants that displayed abnormality in sporulation (Figure 2, Figure 2 – figure supplement 1). We then imaged the wild-type and mutant cells at different time points after glycerol induction and used their length/width (L/W) ratios to monitor potential defects in the sporulation process. Wild-type cells initiated sporulation within 1 h of glycerol induction, which was evidenced by the increase of cell width and decrease of cell length (Figure 2A). Consistent with the change in cell morphology, their L/W ratios decreased continuously and stabilized after 2 h of induction, when sporulation completed. In contrast, the cells that carry the deletion of K1515_20820 (MXAN_RS16290) (Aramayo & Nan, 2022) were able to shorten cell length slightly but retained rod shape after prolonged induction (Figure 2B, Figure 2 – source data 1).

Surprisingly, another mutant that carries the deletion of K1515_17460 (MXAN_RS19615) started to lose rod shape immediately after glycerol induction and became spherical within 1 h (Figure 2A, 2B, Figure 2 – source data 1). However, different from the wild-type spores that appeared dark and heterogeneous under differential interference contrast (DIC) microscopy, the spheres formed by this mutant appeared bright and homogenous, similar to the pseudospores from the *ΔaglQS* mutant that lack the motor for depositing spore coat polysaccharides onto cell surfaces (Zhang et al., 2020) (Figure 2A). To test whether these spheres are real spores, we subjected them to sonication and quantified their survival rate using a Helber bacterial counting chamber. After sonication, while 91 ± 6% (calculated from three independent experiments, n > 1,000) of the wild-type spores appeared intact, only 3 ± 1% of the spheres produced by the K1515_17460 deletion mutant remained. Thus, this mutant indeed formed pseudospores that lacked the resistance against sonication. As the products of K1515_20820 and K1515_17460 show homology to MltE, an LTG encoded by *Escherichia coli emtA* (49.0% and 38.4% sequence identity, respectively) (Figure

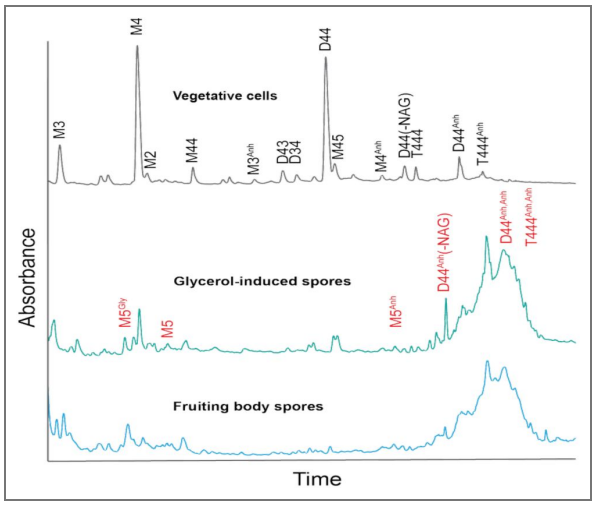

Figure 1. Mature *M. xanthus* spores induced by either glycerol or starvation do not contain significant muropeptides.

UPLC muropeptides profiles of vegetative cells, glycerol- and starvation-induced spores indicate that the major muropeptides species, M4 and D44, in vegetative cells are diminished in both spore types, while spores are enriched in anhydro-muropeptides (Anh). Only muropeptides that could be confidently identified by MS/MS analysis are labelled. The characteristic peaks are labeled as follows: M, monomeric muropeptide (uncrosslinked); D, dimeric muropeptide (crosslink connecting two muropeptides), T, trimeric muropeptide (crosslink connecting three muropeptides). Numbers refer to the status of the peptide side chain (3, tripeptide; 4, tetrapeptide). Red characters mark the muropeptides only detected in spores.

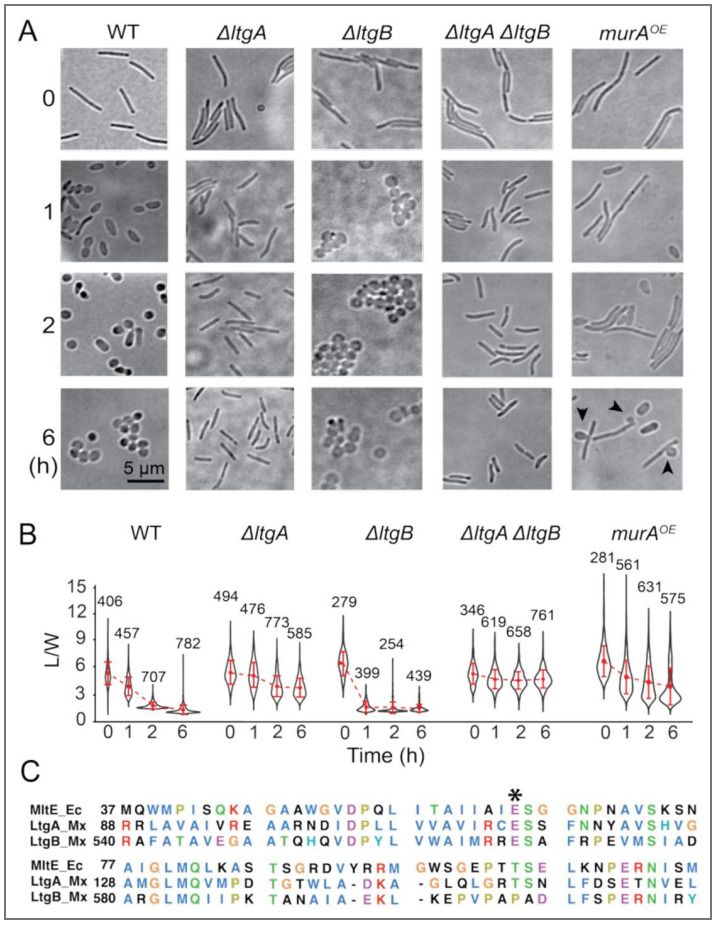

Figure 2. LtgA and LtgB are required for glycerol-induced sporulation, whereas MurA overexpression inhibit sporulation.

A) Bright field images of cells at different time points after glycerol-induction. Black arrows point to lysing cells. **B)** Quantitative analysis of glycerol- induced sporulation using the length/width ratio (L/W) of cells. Whiskers indicate the 25th - 75th percentiles and red dots the median. The total number of cells analyzed is shown on top of each plot. **C)** LtgA and LtgB are homologous to *E. coli* MltE. The asterisk marks the conserved active site. Other putative LTGs do not affect either sporulation pathway significantly, which is shown in Figure 2 – figure supplement 1.

2C), we named them *ltgA* and *ltgB*, respectively. Both LtgA and LtgB are required for forming resistant spores via the rapid sporulation pathway, albeit playing different roles in the rod-to-sphere transition.

To determine if these LTGs are also required for starvation-induced sporulation, we grew them in rich liquid media and spotted cells on solid starvation (CF) media. After 96 h of incubation, both mutants produced dark fruiting bodies on the agar surface that were comparable to those of the wild-type (Figure 3A). To test if these mutants form starvation-induced spores, we incubated cells in static liquid CF medium using polystyrene Petri dishes for 96 h, scraped the cells attached to the dishes, suspended them in 1 ml water, subjected them to sonication, then plated them on solid rich media. After 96 h of incubation, while the wild-type fruiting bodies produced colonies of 3389 ± 1141 cfu/ml (n = 3), the *ΔltgA* and *ΔltgB* cells failed to form colonies after five days of incubation (Figure 3B, Figure 3 – source data 1), indicating that both LtgA and LtgB are essential for forming starvation-induced spores.

LtgA and LtgB play distinct roles in different sporulation pathways

Do LtgA and LtgB degrade PG during sporulation? To answer this question, we purified cell sacculi and used immunofluorescence and an anti-PG serum (de Pedro et al., 1997) to visualize the remaining PG. The sacculi of vegetative cells from the wild- type, *ΔltgA*, and *ΔltgB* strains were not visible under DIC microscopy, likely due to their flattened structures minimizing light interference. However, PG from all three strains was readily detected in the fluorescence channel (Figure 4A). After 6 h of glycerol-induction, the sacculi of both the wild-type and *ΔltgA* cells remained visible under DIC microscopy (Figure 4A), likely due to the deposition of spore coat polysaccharides that sustained unflattened cell structures (Wartel et al., 2013, Holkenbrink et al., 2014). After the sacculus purification process, only background PG signals were detected in glycerol-induced wild-type spores (Figure 4A). In contrast, the *ΔltgA* cells retained PG in substantial quantities (Figure 4A). Sacculi from the *ΔltgB* pseudospores still contained PG but showed lower fluorescence intensity (Figure 4A). While the remaining PG sacculi of these pseudospores were largely spherical, they lost integrity during purification, with many sacculi displaying irregular shapes in the fluorescence channel (Figure 4A). Thus, compared to LtgA, the enzymatic activity of LtgB plays a more limited role in PG degradation during chemical-induced sporulation. Collectively, LtgB appears to be a pace-keeper that prevents abrupt PG degradation. Different from the induced wild-type and *ΔltgA* cells, sacculi from the *ΔltgB* pseudospores were undetectable under DIC microscopy (Figure 4A), reflecting their flattened shapes. This phenotype suggests that further acceleration of the morphological transitions associated with rapid sporulation may impede the formation of a rigid polysaccharide coat.

To determine the roles of LtgA and LtgB in slow sporulation, we first scraped the wild-type fruiting bodies from CF agar surface (Figure 2C), dispersed spores by sonication, purified their sacculi, and visualized PG using immunofluorescence. Spherical spores from the wild-type cells were visible under DIC microscope, indicating that they retained unflattened shapes. These fruiting body spores lacked PG-specific fluorescence (Figure 4A), consistent with their markedly reduced PG content (Figure 1). However, we cannot exclude the possibility that the polysaccharide spore coats (Voelz & Dworkin, 1962) hinder antibody access to PG. Second, we investigated if *ΔltgA* and *ΔltgB* cells degraded PG during starvation-induced sporulation. Because the aggregates formed by *ΔltgA* and *ΔltgB* cells on CF agar did not contain mature spores, we scrapped cell aggregates from agar surface and purified their sacculi without sonication. The *ΔltgA* cells formed spherical, spore-like cells void of PG (Figure 4A), indicating that while LtgB is sufficient for PG degradation during slow sporulation, LtgA is only required for spore maturation. In contrast, most of the *ΔltgB* cells were still rod-shaped, indistinguishable from vegetative ones (Figure 4A). These observations indicate that LtgB is an essential LTG for PG degradation during slow sporulation.

The two sporulation pathways vary greatly in duration: glycerol-induced rapid sporulation is completed within four hours, while starvation-induced slow sporulation unfolds over several days. Based on this distinction, we hypothesized that LtgA and LtgB could degrade PG at different rates. We used a vanillate-inducible promoter (Iniesta et al., 2012) to overexpress LtgA and LtgB

Figure 3. LtgA, LtgB, and MurA regulate starvation-induced sporulation.

A) The absence of LtgA and LtgB, and the overexpression of MurA do not affect the formation of fruiting body– like aggregates on starvation agar. **B)** Both LtgA and LtgB are essential for forming starvation- induced spores, while MurA overexpression negatively regulates this process. Sonication- resistant spores were counted as colony formation units (cfu) after 96 h of incubation on CYE agar. Data are shown as mean ± standard deviation (n = 3).

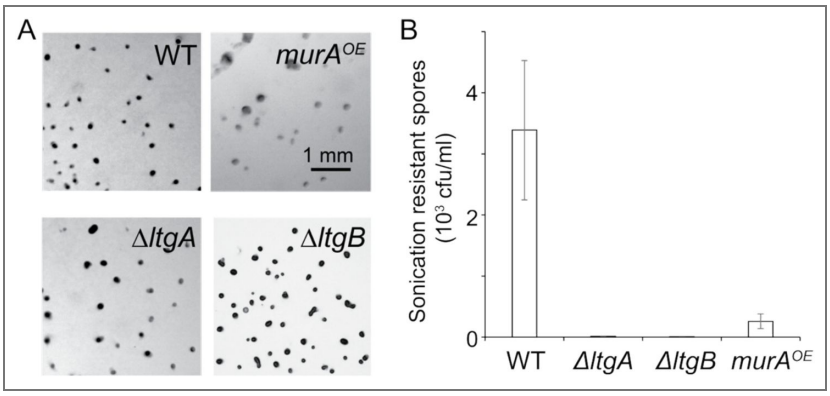

Figure 4. LtgA and LtgB play distinct roles in the two sporulation pathways.

A) While LtgA is required for PG degradation during glycerol-induced sporulation, LtgB is the major LTG for forming starvation-induced spores. PG was detected using an anti-PG serum and a fluorescence-conjugated secondary antibody. PG sacculi were purified from cells after 6 h and 120 h of glycerol-induced and starvation-induced sporulation, respectively. Flattened sacculi are not visible under bright field microscopy. White arrows point to the sacculi in irregular shapes. BF, bright field. **B)** The overexpression of LtgA, but not LtgB, collapses rod-shape in vegetative cells. **C)** Purified LtgA and LtgB solubilize dye-labeled PG sacculi at different rates. Lysozyme and buffer serve as the positive and negative controls, respectively. Absorption at 595 nm was measured after 18 h incubation at 25 ºC. Data are presented as mean values ± SD from three technical replicates. The inset shows purified LtgA and LtgB in a Coomassie stained gel. Scale bars, 5 µm.

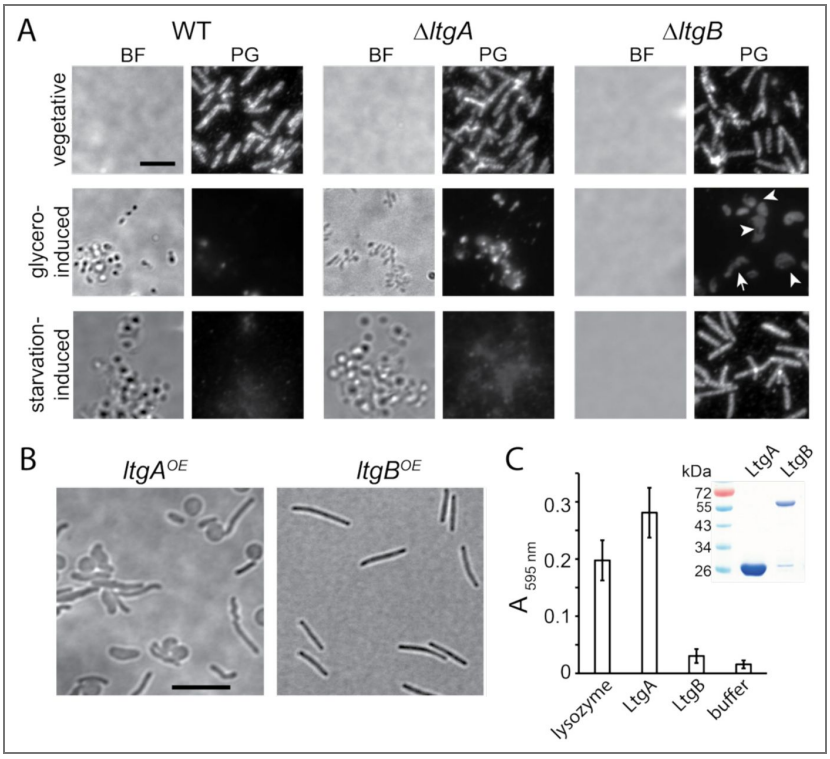

as a merodiploids. Upon induction with 200 μM vanillate, cells overproducing LtgA exhibited heterogeneous morphology, likely resulting from variations in LtgA expression or differences in cell cycle stages within the population. Many cells lost rod shape even in the absence of glycerol, indicating that these cells over-degraded their PG by LtgA (Figure 4B). In contrast, the overexpression of LtgB using the same method did not affect the morphology of vegetative cells (Figure 4B). To test if LtgB overexpression was induced by vanillate, we added a photo-activatable mCherry (PAmCherry) tag to the overexpression constructs of LtgA and LtgB. As shown in Figure 4 – figure supplement 1, in the presence of vanillate, the expression of both LTGs increased significantly. These findings suggest that LtgB exhibits very low LTG activity in vegetative cells, as overexpression of the protein fails to induce substantial PG degradation.

To further investigate the activities of these LTGs, we expressed the periplasmic domains of wild-type LtgA (amino acids 21 – 243) and LtgB (amino acids 26 – 710) in *E. coli* (Figure 4C, Figure 4 – source data 1). We purified PG from wild-type *M. xanthus* cells, labeled it with Remazol brilliant blue (RBB), and tested if the purified LTGs hydrolyze labeled PG *in vitro* and release the dye (Jorgenson et al., 2014, Ramirez Carbo et al., 2024, Uehara et al., 2010). Wild-type LtgA solubilized dye-labeled PG, which absorbed light at 595 nm, demonstrating stronger hydrolytic activity than lysozyme, an enzyme that specifically cleaves β-1,4-glycosidic bonds in PG. In contrast, PG incubated with LtgB only showed minimum release of the dye, indicating slow PG hydrolysis (Figure 4C, Figure 4 – source data 1). While we cannot rule out the possibility that our purification and reaction conditions were suboptimal for LtgB, both the *in vitro* RBB assay and the *in vivo* phenotype resulting from LtgB overexpression support our hypothesis that during vegetative growth, LtgB is less efficient in PG degradation than LtgA.

LtgB regulates LtgA during glycerol-induced sporulation

Consistent with its role in PG degradation, in a microarray-based transcriptome analysis, *ltgA* transcription was found to increase about twofold during rapid sporulation (4 h) but remain unchanged during slow sporulation (96 h) in the closely related DK1622 strain (Muller et al., 2010). Conversely, *ltgB* expression gradually rises during slow sporulation, reaching 1.8 times the vegetative level at 96 h, while remaining stable during rapid sporulation (Muller et al., 2010, Munoz-Dorado et al., 2019). However, transcriptomic data alone do not account for the opposing roles of LtgA and LtgB in the rod-to-sphere transition during rapid sporulation. The resemblance in morphology between glycerol-induced *ΔltgB* cells and uninduced cells overproducing LtgA (Figure 4B) suggests that the slower-acting LtgB may offset the rapid activity of LtgA during sporulation, allowing sufficient time for spore maturation.

To test if LtgB regulates LtgA, we constructed a *ΔltgA ΔltgB* double deletion strain. Cells from this strain shortened their length slightly but failed to abolish rod shape after prolonged glycerol induction, phenocopying the sporulation defect of the *ΔltgA* strain (Figure 2A, 2B, Figure 2 – source data 1). Hence, LtgB is a regulator upstream of LtgA.

LtgB exhibits a response to glycerol induction earlier than LtgA

Biochemical reactions on PG are unique for the stark size difference between the enzymes and their substrates. While the enzymes are in nanometer scales, their substrates, the PG sacculi, span several micrometers. Under the microscope, PG remains stationary but PG-related enzymes are free to move. Even for *M. xanthus* that moves on surfaces, PG-related enzymes move at least two orders of magnitude faster than the cell/PG (Zhang et al., 2023b, Ramirez Carbo et al., 2024). Thus, when diffusive enzymes bind to PG, their mobility decreases (Lee et al., 2016, Zhang et al., 2023b). For instance, DacB, another PG hydrolase, reduces its single-particle mobility in the conditions where its activity is activated (Zhang et al., 2023b). By tracking single fluorescently-labeled enzyme particles, we can approximate their PG-binding in different physiological conditions and genetic backgrounds (Ramirez Carbo et al., 2024, Zhang et al., 2023b, Ramírez Carbó & Nan, 2026). We individually expressed PAmCherry-labeled LtgA and LtgB using their native loci and promoters. Both labeled LTGs accumulated as full- length proteins (Figure 5 – figure supplement 1A) and the PAmCherry tags did not negatively affect either glycerol or starvation-

induced sporulation pathways, indicating that these fusion proteins were fully functional (Figure 5 – figure supplement 1B, C). Notably, vegetative cells produce significantly less LtgA than LtgB, consistent with the RNAseq data in which *ltgA* transcription was below the detection limit (Munoz-Dorado et al., 2019) (Figure 5 – figure supplement 1A).

We used a 405-nm excitation laser (0.3 kW/cm^2, 0.1 s) to activate the fluorescence of a few labeled LTG particles randomly in each cell and quantified their localization using a 561-nm laser at 10 Hz using single particle tracking photo-activated localization microscopy (sptPALM, see Materials and Methods) (Fu et al., 2018, Nan et al., 2015, Nan et al., 2013, Ramírez Carbó & Nan, 2026). As free PAmCherry particles diffuse extremely fast in the cytoplasm, entering and exiting the focal plane frequently, they usually appear as blurry objects that cannot be followed at 10 Hz close to the cell surface (Fu et al., 2018, Zhang et al., 2023b). For this reason, the noise from free PAmCherry due to potential protein degradation was negligible.

Single-particles of PAmCherry-labeled LtgA and LtgB can be categorized into two populations, immobile and mobile. The immobile particles remained within a single pixel (160 nm × 160 nm) before photobleach, and the mobile ones displayed typical diffusion (Figure 5A, Figure 5 – source data 1). For the particles that switched between mobile and immobile states, our algorithm categorized them as mobile and calculated their diffusion coefficients (*D*) from their entire trajectories that contained both mobile and immobile segments. Hence, binding to PG not only increases the immobile population of the enzyme particles but also decreases the *D* of the mobile particles. In vegetative cells where large-scale PG degradation does not occur, 23.9% (n = 1175) and 18.2% (n = 824) of LtgA and LtgB particles were immobile, respectively (Figure 5B, Figure 5 – source data 1). *D* values of the mobile population were (2.62 ± 0.20) × 10^{-2} μm^2/s (n = 894) for LtgA-PAmCherry and (2.80 ± 0.25) × 10^{-2} μm^2/s (n = 674) for LtgB- PAmCherry (Figure 5C, Figure 5 – source data 1).

We then determined how the dynamics of both LTGs respond to glycerol induction in the rapid sporulation pathway. Immediately (1 min) after adding glycerol, the dynamics of LtgA remained little changed, when 21.0% (n = 928) of particles were immobile and the *D* of the mobile ones was (2.53 ± 0.19) × 10^{-2} μm^2/s (n = 733) (Figure 5B, C, Figure 5 – source data 1). In contrast, the mobility of LtgB decreased significantly, with the immobile population increased to 28.0% (n = 1359) and *D* of the mobile population decreased to (2.17 ± 0.28) × 10^{-2} μm^2/s (n = 978) (Figure 5B, C, Figure 5 – source data 1). Therefore, these results suggest that upon glycerol induction, LtgB rapidly enhances its binding to PG.

We then chose 30 min after glycerol induction as a time point for rapid PG degradation, which is reflected by the dramatic decrease of L/W during the first hour of sporulation (Figure 2A, B, Figure 2 – source data 1). Compared to its inert response 1 min after glycerol induction, the mobility of LtgA particles decreased significantly at 30 min, when the immobile population increased to 31.5% (n = 1163) and *D* of the mobile population decreased to (1.80 ± 0.21) × 10^{-2} μm^2/s (n = 797) (Figure 5B, C, Figure 5 – source data 1). The reduced mobility of LtgA aligns with its function as the primary LTG in glycerol-induced sporulation. Strikingly different from LtgA, as sporulation advanced to the 30-min mark, LtgB's mobility returned to its pre-induction level, with the immobile population decreased to 10.2% (n = 1549) and *D* of the mobile population increased to (2.87 ± 0.28) × 10^{-2} μm^2/s (n = 1391) (Figure 5B, C, Figure 5 – source data 1). Therefore, the PG-binding of LtgB shows a negative correlation with PG degradation. Taken together, LtgA and LtgB display opposite responses to glycerol induction, in which LtgB rapidly binds to PG before yielding to LtgA, whose PG-binding is concurrent with the rod-to-sphere transition.

LtgB blocks LtgA from binding PG in the early stage of glycerol-induced sporulation

Does LtgB's early PG-binding suppress PG degradation by LtgA? To answer this question, we expressed LtgA-PAmCherry using the native *ltgA* locus and promoter in the *ΔltgB* background. In vegetative cells, the absence of LtgB significantly reduced the mobility of single LtgA-PAmCherry particles, suggesting that LtgB does affect LtgA's binding to the PG (Figure 5B, C, Figure 5 –

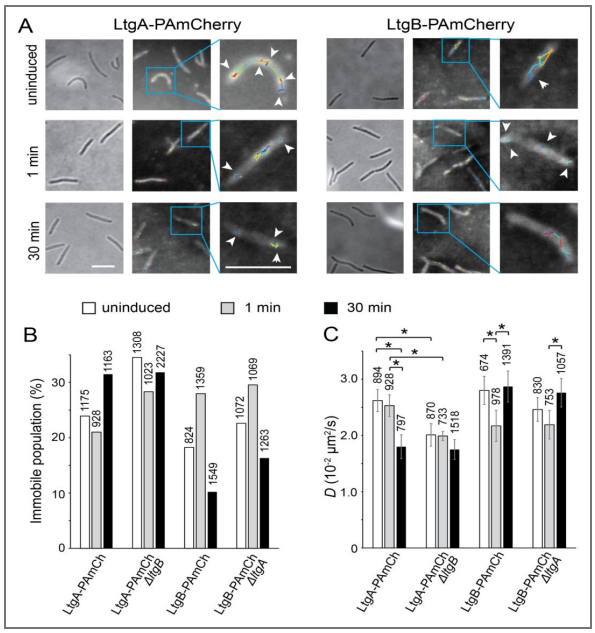

Figure 5. LtgB regulates the PG-binding of LtgA during glycerol-induced sporulation.

A) LtgB exhibits a response to glycerol induction earlier than LtgA. Representative trajectories of LtgA and LtgB before (uninduced) and after (1 min and 30 min) glycerol induction. The overall distribution of both LTGs is displayed using the composite of 100 consecutive frames taken at 100-ms intervals. Single-particle trajectories of PAmCherry were generated from the same frames. Individual trajectories are distinguished by colors. Scale bars, 5 μm. **B** and **C)** the absence of LtgB reduces the diffusion of LtgA, which is reflected in the increase of immobile population (**B**) and the decrease in diffusion coefficient (*D*) (**C**), and these effects are especially prominent in the cells before (uninduced) and immediately after (1 min) glycerol induction. For each protein and condition, particles were identified from at least 100 cells and three independent experiments. The total number of particles analyzed is shown on top of each plot. Error bars were the standard derivation of 1,000 bootstrap samples and * indicates a difference of > 0.005.

source data 1). Similarly, we expressed LtgB- PAmCherry using the native *ltgB* locus and promoter in the *ΔltgA* background. In contrast, the mobility of single LtgB-PAmCherry particles only decreased slightly in the absence of LtgA (Figure 5B, C, Figure 5 – source data 1). These results suggest that while LtgB significantly reduces LtgA's binding to PG, probably due to its higher expression level, LtgA has only a modest impact on LtgB's ability to bind PG.

Strikingly different from its slow response to glycerol in wild-type cells, LtgA increased its PG-binding immediately (1 min) after glycerol induction in the *ΔltgB* background, confirming that LtgB may compete with LtgA for access to PG in the early stage of sporulation (Figure 5B, C, Figure 5 – source data 1). In contrast, at 30 min of induction, a time point when LtgB dissociated from PG, its absence no longer affected LtgA's PG-binding (Figure 5B, C, Figure 5 – source data 1). Similar to the observation in wild-type cells, the lack of LtgA did not affect the PG-binding of LtgB at either 1 min or 30 min after glycerol induction (Figure 5B, C, Figure 5 – source data 1). In summary, the sequential PG-binding by these two LTGs controls the pace of PG-degradation during glycerol-induced sporulation. LtgB, a slow LTG, regulates the progression of rapid sporulation by preventing LtgA, a fast LTG, from excessively degrading PG, thereby ensuring spore maturation.

Upregulated PG synthesis negatively affects PG degradation

Since LtgA is less mobile in vegetative *ΔltgB* cells, i.e. strongly binds to PG (Figure 5B, C, Figure 5 – source data 1), why do these cells retain their rod shape rather than losing it spontaneously before glycerol induction? In addition to PG-binding, LtgA may require additional stimuli to initiate PG degradation. We hypothesized that, similar to certain antibiotics targeting PG synthases, which induce wild-type cells to degrade PG and form pseudospores in rich liquid media (Zhang et al., 2023b, O'Connor & Zusman, 1997), glycerol may alter cellular metabolism, leading to reduced PG synthesis. If this is the case, cells with upregulated PG synthesis should remain rods even in the presence of glycerol.

To test our hypothesis, we used the vanillate-inducible promoter (Iniesta et al., 2012) to overexpress *murA* as a merodiploid in the wild-type background. Because MurA catalyzes the first committed step of PG synthesis that produces UDP-MurNAc (Egan et al., 2020, Rohs & Bernhardt, 2021), elevated MurA levels are expected to channel more cellular resources toward PG synthesis. Overproduction of MurA in the presence of 200 μM vanillate resulted in a heterogeneous cell population, with normal cells coexisting alongside elongated ones (Figure 2A, B, Figure 2 – source data 1). Similar to the cells that overexpressed LtgA (Figure 4B), this heterogeneity likely reflects variable *murA* induction or the unsynchronized growth stages within the population. Overall, excessive MurA increased the average length of vegetative cells by 19.6%. Cells overproducing MurA also displayed heterogeneity during glycerol-induced sporulation. While some cells transitioned into spheres, many retained their rod shape even after 6 h of induction (Figure 2A, B, Figure 2 – source data 1). Notably, sporadic lysis of rod-shaped cells began 2 h post-induction and became increasingly frequent with continued incubation (Figure 2A). Potentially, elevated muropeptide production may lead to the accumulation of toxic intermediates that the relatively insufficient LTGs failed to degrade (Weaver et al., 2022). Nevertheless, the capacity of MurA overexpression to enable certain cells to circumvent glycerol-induced sporulation implies that PG production acts as a regulatory cue for PG degradation.

To test if excessive MurA can also reduce PG degradation during slow sporulation, we induced MurA overexpression on solid CF agar containing 100 μM vanillate. After 96 h of incubation, these cells developed fruiting body-like aggregates (Figure 3A). To test if such fruiting bodies contained mature spores, we scraped them from submerged CF medium and tested the germination rate of spores on CYE agar after sonication. The fruiting bodies formed by cells overexpressing MurA yielded 7.6% of the colonies produced by an equivalent number of wild-type cells, indicating that upregulated PG synthesis also prevents slow sporulation. In contrast, cells grown without vanillate progressed normally through glycerol-induced sporulation and

starvation-induced fruiting body formation, showing no differences compared to wild-type cells (Figure 3B – Figure supplement 2). Therefore, the sporulation of *M. xanthus* is sensitive to PG synthesis and increased PG synthesis balances PG degradation in both sporulation pathways.

Discussion

Our findings demonstrate that *M. xanthus*, a non-firmicute bacterium, relies on PG degradation to change cell shape during sporulation. This mechanism presents a significant challenge for sporulating cells: preserving their structural integrity while simultaneously dismantling the primary framework that upholds it. Our findings revealed that besides regulating the production of LTGs, cells could control the pace of PG degradation in a rapid sporulation pathway through the regulation between two LTGs and hence allow spore maturation.

Studying the regulation between two LTGs is especially challenging both *in vivo* and *in vitro* for a few reasons. First, it is difficult to monitor their instantaneous activities *in vivo*. Secondly, muropeptide analysis may not distinguish their roles because their products bear the same signature, anhydro-MurNAc. Thirdly, some enzymes require special substrates or activators, which would be difficult to study *in vitro*. To overcome these technical hurdles, we leveraged single-particle mobility to quantify the PG- binding of these enzymes. The simultaneous occurrence of reduced LtgA mobility and PG degradation during glycerol-induced sporulation indicates that the molecular dynamics of LtgA accurately mirrors its enzymatic activity. Such correlation between decreased particle mobility and increased enzymatic activity applies to many other PG- related enzymes, including multiple PG polymerases in *E. coli* and the endopeptidase DacB in *M. xanthus* (Lee et al., 2016, Zhang et al., 2023b, Yang et al., 2021). Because the size difference between PG and its related enzymes is a conserved feature in all bacteria, our method using single-particle tracking to quantify PG-binding can be applied in many organisms.

We discovered that LtgB, a slower-acting LTG, limits the access of the faster LtgA to the PG during the early phase of rapid sporulation, thereby regulating the rate of its degradation. Then how does LtgA breach the blockage of LtgB and gain access to PG as sporulation progresses? Because the overexpression of LtgA is sufficient to damage PG in uninduced cells (Figure 4B), we propose that the relative abundance of these two LTGs plays a critical role in determining the fate during fast sporulation. While LtgB nearly saturates PG binding sites in vegetative cells where few LtgA are produced, LtgA—upregulated after glycerol induction (Muller et al., 2010) —gradually outcompetes LtgB and thereby causes LtgB to disassociate from PG.

As increased PG synthesis enables many cells to bypass both sporulation pathways, it is reasonable to propose that diminished PG synthesis initiates PG degradation by LTGs. While functional coordination between PG synthesis and hydrolysis has been speculated for over 50 years (Koch, 1985, Koch, 1990), its mechanisms only came to light recently. Some endopeptidases are proposed to serve as the space-makers for PG synthases (Dorr et al., 2013, Singh et al., 2012). In *M. xanthus*, we reported that moenomycin, an antibiotic that specifically binds to the GTase domains of class A penicillin-binding proteins (aPBPs) (Sung et al., 2009, Lovering et al., 2007), specifically activates a PG endopeptidase DacB through PBP1a2, an aPBP (Zhang et al., 2023b). Because moenomycin mimics a growing glycan strand in the GTase domains of aPBPs, it actually locks aPBPs in their glycan-charged conformations (Sung et al., 2009, Lovering et al., 2007). Thus, similar to the moenomycin-bound form, glycan-charged PBP1a2 in physiological conditions recruits DacB to the PG assembly sites, which in turn, generates openings in the existing PG network as the crosslink sites for the TPase activity of PBP1a2. Such “make-before-break” mechanism (Koch & Doyle, 1985) could prevent unneeded hydrolysis and thus maintain PG integrity.

Compared to the well-characterized space-making functions of endopeptidases, the roles of LTGs, beyond PG recycling, remain ill-defined. Even less is known on their potential coordination with PG synthases (Weaver et al., 2023). Because LTGs from bacterial and phage origins are inhibited by L,D-crosslinks, they may functionally connect to PBPs that form D,D-crosslinks (Alvarez et al., 2024). Additionally, some LTGs, such as MltD and MltG in *E. coli* and MltG in *Vibrio cholerae*,

prefer to degrade nascent, uncrosslinked glycan strands (Kaul et al., 2024, Weaver et al., 2022, Bohrhunter et al., 2021). Our recent report indicates that AgmT, an *M. xanthus* LTG homologous to *E. coli* MltG, detoxifies uncrosslinked glycan strands under antibiotic stress and modifies crosslinked PG scaffolds to attach a motility machinery to PG (Ramirez Carbo et al., 2024). Then how does reduced PG synthesis activate LtgA in *M. xanthus*? Although MltE, the closest homolog of LtgA in *E. coli*, degrades glycan strands regardless of their crosslinking status or peptide content, it shows a marked preference for uncrosslinked substrates (Dik et al., 2017, Fibriansah et al., 2012). Similar to AgmT and MltE, LtgA might also bind to both crosslinked and uncrosslinked glycan strands. Consistent with its high mobility, LtgA may coordinate with diffusive PG polymerases and cleave the uncrosslinked glycan strands. During rapid sporulation, as nascent glycan strands decline due to muropeptide depletion, LtgA increasingly binds to the crosslinked PG scaffold, which is evidenced by its reduced mobility. This binding intensifies further as PG degradation continues, establishing a positive feedback loop. In this case, LtgB serves as a brake that dampens this positive feedback, moderates PG degradation, and thus allows sporulating cells to maintain integrity by assembling polysaccharide coats. Such cross-regulation between PG hydrolases, which is currently under investigation, provides yet another mechanism by which bacteria dynamically maintain their PG cell walls.

Materials and Methods

Bacterial strains and growth conditions

Vegetative *M. xanthus* cells were grown in liquid CYE medium (10 mM MOPS pH 7.6, 1% (w/v) Bacto™ casitone (BD Biosciences), 0.5% yeast extract and 8 mM $MgSO_4$) at 32 °C, in 125-ml flasks with vigorous shaking, or on CYE plates that contains 1.5% agar. We used strain DZ2 as the wild-type *M. xanthus* strain (Campos & Zusman, 1975). Knock-out mutants were constructed by electroporating DZ2 cells with 4 μg of plasmid DNA. Transformed cells were plated on CYE plates supplemented with 100 mg/ml sodium kanamycin sulfate or 10 mg/ml tetracycline. The strains and plasmids used in this study are listed in Table 1.

Sporulation and spore purification

Cells were grown in 25 ml liquid cell culture to OD_{600} 0.8 – 1.2. Glycerol was added to 1 M to induce sporulation. The liquid culture was incubated at 32 °C with vigorous shaking. After 24 h, spores and cells were harvested by centrifugation (10 min, 10,000 g and 25 °C). To further purify the wild-type spores, the pellet was resuspended in 5 ml water, the remaining vegetative cells were eliminated by sonication (Cole Palmer 4710 ultrasonic homogenizer, 30% output, 10 cycles), and sonication-resistant spores were washed three times with water and collected by centrifugation (5 min, 10,000 *g* and 4 °C). The elimination of vegetative cells was confirmed by DIC microscopy.

For phenotypic assays on starvation-induced fruiting body formation, vegetative cells (10 ul), at a concentration of 4×10^9 ml^{-1}, were spotted on CF (0.015% Casitone, 0.2% sodium citrate, 0.1% sodium pyruvate, 0.02% $(NH_4)_2SO_4$, 10 mM MOPS (pH 7.6), 8 mM $MgSO_4$ and 1 mM KH_2PO_4) plates containing an agar concentration of 1.5%, incubated at 32°C. To purify fruiting body spores, cells were grown in 25 ml liquid cell culture to OD_{600} 0.8 – 1.2 and harvested by centrifugation (10 min, 10,000 g and 25 °C). The pellet was resuspended in 1 ml water and plated on two 150 mm CF plates containing 1.5% agar using a spreader. The plates were air-dried and incubated at 32 °C for 120 h. For the wild-type and *ΔltgA* strains, fruiting bodies were scraped from the plates, suspended in 2 ml water, and subjected to sonication (Cole Palmer 4710 ultrasonic homogenizer, 60% output, 20 cycles). Spores were washed three times in water and collected by centrifugation (5 min, 10,000 g and 4 °C). For the *ΔltgB* strains, the sonication step was omitted.

Table 1. **Strains and plasmids used in this study**

***M. xanthus* Strain**	**Description**	**Source**
DZ2	The wild-type strain	(Campos & Zusman, 1975)
BN361	*ΔltgA*	This study
BN362	*ΔltgB*	This study
BN363	*ΔltgA ΔltgB*	This study
BN364	*ΔltgA pMR3629-ltgB*	This study
BN365	DZ2 with P_{van}-*ltgA*	This study
BN366	DZ2 with P_{van}-*ltgB*	This study
BN367	DZ2 with P_{van}-*ltgA-PAmCherry*	This study
BN368	DZ2 with P_{van}-*ltgB-PAmCherry*	This study
BN369	DZ2 with P_{van}-*murA*	This study
BN370	*ltgA-PAmCherry*	This study
BN371	*ltgB-PAmCherry*	This study
BN372	*ΔltgB ltgA-PAmCherry*	This study
BN373	*ΔltgA ltgB-PAmCherry*	This study
***E. coli* Strain**	**Description**	**Source**
DH5α	*E. coli* strain for molecular cloning	lab collection
BL31 (DE3)	*E. coli* host for protein expression	Novagen
Plasmid name	**Description**	**Source**
pMR3629	Plasmid for overexpressing genes as merodiploids using a vanilate-induced promoter, tet^R	(Iniesta *et al.*, 2012)
pMR3629-*ltgA*	P_{van}-*ltgA* in pMR3629, tet^R	This study
pMR3629-*ltgB*	P_{van}-*ltgB* in pMR3629, tet^R	This study
pMR3629-*ltgA*	P_{van}-*ltgA-PAmCherry* in pMR3629, tet^R	This study
pMR3629-*ltgB*	P_{van}-*ltgB-PAmCherry* in pMR3629, tet^R	This study
pMR3629-*murA*	P_{van}-*murA* in pMR3629, tet^R	This study
pET28a-*ltgA*	Plasmid for overexpression of His-tagged LtgA, kan^R	This study
pET28a-*ltgB*	Plasmid for overexpression of His-tagged LtgB, kan^R	This study

Quantification of starvation-induced spores

We used the submerge starvation culture to quantify starvation-induced spores. Cells were first grown in liquid CYE medium overnight and adjusted to OD_{600} 1 using fresh CYE. 50 ml of the asjusted culture was then poured to a Ø 150 mm polystyrene Petri dish and incubated without shaking for 24 h at 32 °C. Liquid and unattached cells were poured out carefully before adding 50 ml liquid CF medium. Petri dished were incubated without shaking for 96 h at 32 °C. Finally, liquid and unattached cells were poured out carefully and the cells attached to the bottom of Petri dished were scraped and resuspened into 1 ml water. The suspensions were then sonicated to eliminate vegetative cells, diluted and plated on solid CYE medium. Sonication-resistant spores were then numerated by counting the colonies after a 96-h incubation at 32 °C. Data were collected using three biological replicates.

Peptidoglycan purification and UPLC analysis

For PG analysis, samples were processed as previously described for Gram negative bacteria (Alvarez et al., 2016, Desmarais et al., 2013). Vegetative cells were harvested at mid-stationary phase by centrifugation (30 min, 8,000 g). Vegetative cells and purified spores (as described in the previous section) were resuspended and boiled in 1x PBS with 5% SDS for 2 h. The sacculi were repeatedly washed with MilliQ water by ultracentrifugation (150,000 g, 10 min, 20 °C) to remove the remaining SDS. The samples were then treated with muramidase (100 µg/mL) for 16 hours at 37 °C. Muramidase digestion was stopped by boiling and coagulated proteins were removed by centrifugation (10 min, 15,000 g). The supernatants were first adjusted to pH 8.5-9.0 with sodium borate buffer and then sodium borohydride was added to a final concentration of 10 mg/ml. After reducing the samples at room temperature for 30 min, the pH was adjusted to pH 3.5 with orthophosphoric acid.

UPLC analyses of muropeptides were performed on a Waters UPLC system (Waters Corp., USA) equipped with an ACQUITY UPLC BEH C18 Column (Waters Corp., USA) and a dual wavelength absorbance detector. Elution of muropeptides was detected at 204 nm. Muropeptides were separated at 45 °C using a linear gradient from buffer A (0.1% formic acid in water) to buffer B (0.1% formic acid in acetonitrile) in a 25- min run, with a 0.30 ml/min flow.

Muropeptide identification

Muropeptide identity was confirmed by MS and MS/MS analysis on a Xevo G2/XS Q- TOF mass spectrometer (Waters Corp., USA) coupled to the UPLC system with the same column, solvents, and gradients as mentioned above. Data acquisition and processing were performed using the UNIFI software package (Waters Corp., USA). Muropeptides were assigned based on: (i) accurate mass matching to theoretical monoisotopic masses of expected *M. xanthus* PG building blocks (Bui et al., 2009, White et al., 1968) and (ii) comparison of retention times with those reported in previous analysis with similar PG compositions. For vegetative cells analysis, relative total PG amounts were calculated by comparison of the total intensities of the chromatograms (total area) from three biological replicas normalized to the same initial biomass and extracted with the same volumes. Quantification of muropeptides was based on their relative abundances (relative area of the corresponding peak).

Imaging and data analysis

For all imaging experiments on isolated spores/cells, we spotted 5 µl of cells grown in liquid CYE medium to OD_{600} ~1 on agar (1.5%) pads and imaged using a Andor iXon Ultra 897 EMCCD camera (effective pixel size 160 nm) on an inverted Nikon Eclipse- Ti™ microscope with a 100× 1.49 NA TIRF objective. Fruiting bodies were photographed after a 120-h incubation on CF agar using a Nikon SMZ1000 microscope and an OMAX A3590U digital camera. Cell morphology was imaged at indicated time points using DIC microscopy. The geometric aspect ratios (L/W) of spores/cells were

determined using a custom algorithm written in MATLAB, which is available in the GitHub repository, *https://github.com/NanLabMyxo/Rod_shape_paper* (Zhang et al., 2020, Zhang et al., 2023a, Zhang et al., 2023b).

For sptPALM, *M. xanthus* cells were grown in CYE to 4 ×10^8 ml, spotted on 1.5% agar pads and subjected to highly inclined and laminated optical sheet (HILO) illumination (Fu et al., 2018, Nan et al., 2015, Nan et al., 2013, Tokunaga et al., 2008). PAmCherry was activated using a 405-nm laser (0.3 kW/cm^2), excited and imaged using a 561-nm laser (0.2 kW/cm^2). Images were acquired at 10 Hz. For each sptPALM experiment, single PAmCherry particles were localized in at least 100 individual cells from three biological replicates. sptPALM data were analyzed using a MATLAB (MathWorks) script, which is available in the GitHub repository, *https://github.com/NanLabMyxo/Rod_shape_paper* (Zhang et al., 2020, Zhang et al., 2023a, Zhang et al., 2023b, Ramírez Carbó & Nan, 2026). Briefly, cells were identified using differential interference contrast images. Single PAmCherry particles inside cells were fit by a symmetric 2D Gaussian function, whose center was assumed to be the particle's position (Fu et al., 2018). Particles that explored areas smaller than 160 nm × 160 nm (within one pixel) in 0.4 - 1.2 s were considered immotile (Fu et al., 2018, Zhang et al., 2023a, Zhang et al., 2023b). *D* of all the mobile particles was determined from a linear fit to the first four points of the MSD using a formula MSD = $4D\Delta t$ (Fu et al., 2018, Lee et al., 2016). Error bars were the standard derivation of 1,000 bootstrap samples using the published method (Morgenstein et al., 2015). Sample trajectories were generated using the TrackMate (Ershov et al., 2022) plugin in the ImageJ suite (*https://imagej.net*).

Immunofluorescence

Cell samples were resuspended and boiled in 1x PBS with 5% SDS for 2 h. The sacculi were repeatedly washed with water by centrifugation (5 min, 15,000 g and 25 °C) to remove the remaining SDS. Remaining proteins were further removed by incubation with proteinase K (1 µg/ml) for 2 h at 37 °C. Microscope cover slides were prepared by coating with 100 µl 0.1% poly-L-lysine for 5 min at room temperature (RT), washing with ddH_2O and air drying. 100 µl samples were spotted onto the slides and incubated for 20 min at RT. The slides were then washed three times with phosphate buffer saline (PBS; 81 mM Na_2HPO_4, 15 mM KH_2PO_4, 1.37 M NaCl, 27 mM KCl, pH 7.4), and then incubated with anti-PG primary antibody[16] diluted 1:1000 in PBS at RT for 1 h. Slides were washed 6 times with PBS and then incubated with Alexa Fluor 488 conjugated goat-anti-rabbit secondary antibody (Invitrogen) at a 1:1000 dilution in PBS at RT for 1 h in the dark. Slides were washed 6 times with PBS. Each cover glass was applied to a supporting slide, fixed with nail polish, and stored at 4 °C, if necessary. Images were recorded using a 488-nm laser.

Protein expression and purification

DNA sequences encoding amino acids 21 – 243 of LtgA and 26 - 710 of LtgB were amplified by polymerase chain reaction (PCR) and inserted into the pET28a vector (Novagen) between the restriction sites of *Eco*RI and *Hind*III and used to transform *E. coli* strain BL21(DE3). Transformed cells were cultured in 20 ml LB (Luria-Bertani) broth at 37 °C overnight and used to inoculate 1 L LB medium supplemented with 1.0% glucose. Protein expression was induced by 0.1 mM IPTG (isopropyl-h-d- thiogalactopyranoside) when the culture reached an OD_{600} of 0.8. Cultivation was continued at 16 °C for 10 h before the cells were harvested by centrifugation at 6,000 × g for 20 min and lysed by sonication in buffer A (20 mM Tris-HCl pH 8.0, 200 mM NaCl), (Nan et al., 2010, Nan et al., 2006). Proteins were loaded to an NGC™ Chromatography System (BIO-RAD) and 5-ml HisTrap™ columns (Cytiva) and eluted by buffer B (20 mM Tris-HCl pH 8.0, 200 mM NaCl, 500 mM immidazole) (Pogue et al., 2018, Nan et al., 2010). Purified proteins were concentrated using Amicon™ Ultra centrifugal filter units (Millipore Sigma) with a 10-kDa molecular weight cutoff and stored at −80 °C.

LTG activity (RBB) assay

PG was purified following the published method (Zhang et al., 2023b, Alvarez et al., 2016, Ramirez Carbo et al., 2024). In brief, *M. xanthus* cells were grown until mid- stationary phase and harvested by centrifugation (6,000 × g, 20 min, 25 °C). Supernatant was discarded and the pellet was resuspended and boiled in 1× PBS with 5% SDS for 2 h. SDS was removed by repetitive wash with water and centrifugation (21,000 × g, 10 min, 25 °C). Purified PG from 100 ml culture was suspended into 1 ml 1× PBS and stored at −20 °C. RBB labelling of PG was performed essentially as previously described (Uehara et al., 2010, Jorgenson et al., 2014). Purified sacculi were incubated with 20 mM RBB in 0.25 M NaOH overnight at 37 °C. Reactions were neutralized by adding equal volumes of 0.25 M HCl and RBB-labeled PG was collected by centrifugation at 21,000 × g for 15 min. Pellets were washed repeatedly with water until the supernatants became colorless. RBB-labelled sacculi were incubated with purified LtgA or LtgB (1 mg/ml) at 25 °C for 12 h. lysozyme (1 mg/ml) was used as a positive control. Dye release was quantified by the absorption at 595 nm from the supernatants after centrifugation (21,000 × g, 10 min, 25 °C).

Immunoblotting

Cells were grown in liquid CYE medium overnight, harvested, and concentrated to OD_{600} 10. 10 µl of cell suspension was mixed with 10 µl of loading buffer and 10 µl of the mixture was subjected to SDS-PAGE. The expression and stability of PAmCherry- labeled proteins were determined by immunoblotting using an anti-mCherry antibody (Rockland Immunochemicals, Inc., Lot 46705) and a goat anti-Rabbit IgG (H+L) secondary antibody, HRP (Thermo Fisher Scientific, catalog # 31460). MreB was detected as the loading control using an anti-MreB serum(Mauriello et al., 2010) and the same secondary antibody. The blots were developed with Pierce™ ECL Western Blotting Substrate (Thermo Fisher Scientific REF 32109) and a MINI-MED 90 processor (AFP Manufacturing).

Data availability

Figure 2-source data 1, Figure 3-source data 1, Figure 4-source data 1, and Figure 5-source data 1 contain the numerical data used to generate the figures.

Acknowledgements

This work was supported by the National Institutes of Health grants GM129000 to B. N. Research in the F. C. laboratory is supported by the Swedish Research Council, the Laboratory for Molecular Infection Medicine Sweden (MIMS), Umeå University, the Knut and Alice Wallenberg Foundation (KAW) and the Kempe Foundation. B. N.'s group received financial support from Dr. David R. Zusman, who played no role in the design, execution, or presentation of this work.

Additional files

Supplementary file 1. Figure supplements.

Figure 1 - Source data 1.

Figure 3 - Source data 1.

Figure 4 - Source data 1.

Figure 5 - Source data 1.

Additional information

Author ORCID iDs

Felipe Cava: https://orcid.org/0000-0001-5995-718X
Beiyan Nan: https://orcid.org/0000-0002-0326-9529

References

Alvarez L, Hernandez SB, de Pedro MA, Cava F (2016) Ultra-Sensitive, High-Resolution Liquid Chromatography Methods for the High-Throughput Quantitative Analysis of Bacterial Cell Wall Chemistry and Structure. *Methods Mol Biol* **1440**:11-27 https://doi.org/10.1007/978-1-4939-3676-2_2 | PubMed

Alvarez L, Hernandez SB, Torrens G, Weaver AI, Dorr T, Cava F (2024) Control of bacterial cell wall autolysins by peptidoglycan crosslinking mode. *Nature communications* **15**:7937 https://doi.org/10.1038/s41467-024-52325-2 | PubMed

Aramayo R, Nan B (2022) *De Novo* Assembly and Annotation of the Complete Genome Sequence of *Myxococcus xanthus* DZ2. *Microbiol Resour Announc* e0107421 https://doi.org/10.1128/mra.01074-21 | PubMed

Bohrhunter JL, Rohs PDA, Torres G, Yunck R, Bernhardt TG (2021) MltG activity antagonizes cell wall synthesis by both types of peptidoglycan polymerases in *Escherichia coli*. *Mol Microbiol* **115**:1170-1180 https://doi.org/10.1111/mmi.14660 | PubMed

Bui NK, Gray J, Schwarz H, Schumann P, Blanot D, Vollmer W (2009) The peptidoglycan sacculus of *Myxococcus xanthus* has unusual structural features and is degraded during glycerol- induced myxospore development. *J Bacteriol* **191**:494-505 https://doi.org/10.1128/jb.00608-08 | PubMed

Campos JM, Zusman DR (1975) Regulation of Development in *Myxococcus-xanthus* - Effect of 3' Doublebond 5'-Cyclic Amp, Adp, and Nutrition. *Proceedings of the National Academy of Sciences of the United States of America* **72**:518-522 https://doi.org/10.1073/pnas.72.2.518 | PubMed

de Pedro MA, Quintela JC, Holtje JV, Schwarz H (1997) Murein segregation in *Escherichia coli*. *J Bacteriol* **179**:2823-2834 https://doi.org/10.1128/jb.179.9.2823-2834.1997 | PubMed

Desmarais SM, De Pedro MA, Cava F, Huang KC (2013) Peptidoglycan at its peaks: how chromatographic analyses can reveal bacterial cell wall structure and assembly. *Mol Microbiol* **89**:1-13 https://doi.org/10.1111/mmi.12266 | PubMed

Dik DA, Marous DR, Fisher JF, Mobashery S (2017) Lytic transglycosylases: concinnity in concision of the bacterial cell wall. *Crit Rev Biochem Mol Biol* **52**:503-542 https://doi.org/10.1080/10409238.2017.1337705 | PubMed

Dorr T, Cava F, Lam H, Davis BM, Waldor MK (2013) Substrate specificity of an elongation- specific peptidoglycan endopeptidase and its implications for cell wall architecture and growth of *Vibrio cholerae*. *Mol Microbiol* **89**:949-962 https://doi.org/10.1111/mmi.12323 | PubMed

Dworkin M, Gibson SM (1964) A System for Studying Microbial Morphogenesis: Rapid Formation of Microcysts in *Myxococcus xanthus*. *Science* **146**:243-244 https://doi.org/10.1126/science.146.3641.243 | PubMed

Egan AJF, Errington J, Vollmer W (2020) Regulation of peptidoglycan synthesis and remodelling. *Nat Rev Microbiol* **18**:446-460 https://doi.org/10.1038/s41579-020-0366-3 | PubMed

Ershov D, Phan MS, Pylvanainen JW, Rigaud SU, Le Blanc L, Charles-Orszag A, Conway JRW, Laine RF, Roy NH, Bonazzi D, *et al.* (2022) TrackMate 7: integrating state-of-the-art segmentation algorithms into tracking pipelines. *Nat Methods* **19**:829-832 https://doi.org/10.1038/s41592-022-01507-1 | PubMed

Fibriansah G, Gliubich FI, Thunnissen AM (2012) On the mechanism of peptidoglycan binding and cleavage by the endo-specific lytic transglycosylase MltE from *Escherichia coli*. *Biochemistry* **51**:9164-9177 https://doi.org/10.1021/bi300900t | PubMed

Fu G, Bandaria JN, Le Gall AV, Fan X, Yildiz A, Mignot T, Zusman DR, Nan B (2018) MotAB-like machinery drives the movement of MreB filaments during bacterial gliding motility. *Proc Natl Acad Sci U S A* **115**:2484-2489 https://doi.org/10.1073/pnas.1716441115 | PubMed

Higgins D, Dworkin J (2012) Recent progress in *Bacillus subtilis* sporulation. *FEMS Microbiol Rev* **36**:131-148 https://doi.org/10.1111/j.1574-6976.2011.00310.x | PubMed

Holkenbrink C, Hoiczyk E, Kahnt J, Higgs PI (2014) Synthesis and assembly of a novel glycan layer in *Myxococcus xanthus* spores. *J Biol Chem* **289**:32364-32378 https://doi.org/10.1074/jbc.m114.595504 | PubMed

Huang M, Hull CM (2017) Sporulation: how to survive on planet Earth (and beyond). *Curr Genet.* https://doi.org/10.1007/s00294-017-0694-7 | PubMed

Hutchison EA, Miller DA, Angert ER (2014) Sporulation in Bacteria: Beyond the Standard Model. *Microbiol Spectr* **2** https://doi.org/10.1128/microbiolspec.tbs-0013-2012 | PubMed

Iniesta AA, Garcia-Heras F, Abellon-Ruiz J, Gallego-Garcia A, Elias-Arnanz M (2012) Two systems for conditional gene expression in *Myxococcus xanthus* inducible by isopropyl-beta-D-thiogalactopyranoside or vanillate. *J Bacteriol* **194**:5875-5885 https://doi.org/10.1128/jb.01110-12 | PubMed

Jorgenson MA, Chen Y, Yahashiri A, Popham DL, Weiss DS (2014) The bacterial septal ring protein RlpA is a lytic transglycosylase that contributes to rod shape and daughter cell separation in *Pseudomonas aeruginosa*. *Mol Microbiol* **93**:113-128 https://doi.org/10.1111/mmi.12643 | PubMed

Kaul M, Meher SK, Nallamotu KC, Reddy M (2024) Glycan strand cleavage by a lytic transglycosylase, MltD contributes to the expansion of peptidoglycan in *Escherichia coli*. *PLoS Genet* **20**:e1011161 https://doi.org/10.1371/journal.pgen.1011161 | PubMed

Koch AL (1985) How Bacteria Grow and Divide in Spite of Internal Hydrostatic-Pressure. *Canadian Journal of Microbiology* **31**:1071-1084 https://doi.org/10.1139/m85-204 | PubMed

Koch AL (1990) Additional arguments for the key role of "smart" autolysins in the enlargement of the wall of gram-negative bacteria. *Res Microbiol* **141**:529-541 https://doi.org/10.1016/0923-2508(90)90017-k | PubMed

Koch AL, Doyle RJ (1985) Inside-to-outside growth and turnover of the wall of gram-positive rods. *J Theor Biol* **117**:137-157 https://doi.org/10.1016/s0022-5193(85)80169-7 | PubMed

Kottel RH, Bacon K, Clutter D, White D (1975) Coats from *Myxococcus xanthus*: characterization and synthesis during myxospore differentiation. *J Bacteriol* **124**:550-557 https://doi.org/10.1128/jb.124.1.550-557.1975 | PubMed

Kroos L, Wall D, Islam ST, Whitworth DE, Munoz-Dorado J, Higgs PI, Singer M, Mauriello EM, Treuner-Lange A, Sogaard-Andersen L, *et al.* (2025) Milestones in the development of *Myxococcus xanthus* as a model multicellular bacterium. *J Bacteriol* **207**:e0007125 https://doi.org/10.1128/jb.00071-25 | PubMed

Lee TK, Meng K, Shi H, Huang KC (2016) Single-molecule imaging reveals modulation of cell wall synthesis dynamics in live bacterial cells. *Nature communications* **7**:13170 https://doi.org/10.1038/ncomms13170 | PubMed

Lovering AL, de Castro LH, Lim D, Strynadka NC (2007) Structural insight into the transglycosylation step of bacterial cell-wall biosynthesis. *Science* **315**:1402-1405 https://doi.org/10.1126/science.1136611 | PubMed

Mauriello EM, Mouhamar F, Nan B, Ducret A, Dai D, Zusman DR, Mignot T (2010) Bacterial motility complexes require the actin-like protein, MreB and the Ras homologue, MglA. *Embo J* **29**:315-326 https://doi.org/10.1038/emboj.2009.356 | PubMed

McKenney PT, Eichenberger P (2012) Dynamics of spore coat morphogenesis in *Bacillus subtilis*. *Mol Microbiol* **83**:245-260 https://doi.org/10.1111/j.1365-2958.2011.07936.x | PubMed

Morgenstein RM, Bratton BP, Nguyen JP, Ouzounov N, Shaevitz JW, Gitai Z (2015) RodZ links MreB to cell wall synthesis to mediate MreB rotation and robust morphogenesis. *Proc Natl Acad Sci U S A* https://doi.org/10.1073/pnas.1509610112 | PubMed

Muller FD, Schink CW, Hoiczyk E, Cserti E, Higgs PI (2012) Spore formation in *Myxococcus xanthus* is tied to cytoskeleton functions and polysaccharide spore coat deposition. *Mol Microbiol* **83**:486-505 https://doi.org/10.1111/j.1365-2958.2011.07944.x | PubMed

Muller FD, Treuner-Lange A, Heider J, Huntley SM, Higgs PI (2010) Global transcriptome analysis of spore formation in *Myxococcus xanthus* reveals a locus necessary for cell differentiation. *BMC Genomics* **11**:264 https://doi.org/10.1186/1471-2164-11-264 | PubMed

Munoz-Dorado J, Moraleda-Munoz A, Marcos-Torres FJ, Contreras-Moreno FJ, Martin-Cuadrado AB, Schrader JM, Higgs PI, Perez J (2019) Transcriptome dynamics of the *Myxococcus xanthus* multicellular developmental program. *eLife* **8** https://doi.org/10.7554/elife.50374 | PubMed

Nan B, Bandaria JN, Guo KY, Fan X, Moghtaderi A, Yildiz A, Zusman DR (2015) The polarity of myxobacterial gliding is regulated by direct interactions between the gliding motors and the Ras homolog MglA. *Proc Natl Acad Sci U S A* **112**:E186-193 https://doi.org/10.1073/pnas.1421073112 | PubMed

Nan B, Bandaria JN, Moghtaderi A, Sun IH, Yildiz A, Zusman DR (2013) Flagella stator homologs function as motors for myxobacterial gliding motility by moving in helical trajectories. *Proc Natl Acad Sci U S A* **110**:E1508-1513 https://doi.org/10.1073/pnas.1219982110 | PubMed

Nan B, Liu X, Zhou Y, Liu J, Zhang L, Wen J, Zhang X, Su XD, Wang YP (2010) From signal perception to signal transduction: ligand-induced dimeric switch of DctB sensory domain in solution. *Mol Microbiol* **75**:1484-1494 https://doi.org/10.1111/j.1365-2958.2010.07069.x | PubMed

Nan B, Zhou Y, Liang YH, Wen J, Ma Q, Zhang S, Wang Y, Su XD (2006) Purification and preliminary X-ray crystallographic analysis of the ligand-binding domain of *Sinorhizobium meliloti* DctB. *Biochim Biophys Acta* **1764**:839-841 https://doi.org/10.1016/j.bbapap.2005.10.023 | PubMed

O'Connor KA, Zusman DR (1988) Reexamination of the role of autolysis in the development of *Myxococcus xanthus*. *J Bacteriol* **170**:4103-4112 https://doi.org/10.1128/jb.170.9.4103-4112.1988 | PubMed

O'Connor KA, Zusman DR (1997) Starvation-independent sporulation in *Myxococcus xanthus* involves the pathway for beta-lactamase induction and provides a mechanism for competitive cell survival. *Mol Microbiol* **24**:839-850 https://doi.org/10.1046/j.1365-2958.1997.3931757.x | PubMed

Perez-Burgos M, Garcia-Romero I, Valvano MA, Sogaard Andersen L (2020) Identification of the Wzx flippase, Wzy polymerase and sugar-modifying enzymes for spore coat polysaccharide biosynthesis in *Myxococcus xanthus*. *Mol Microbiol* **113**:1189-1208 https://doi.org/10.1111/mmi.14486 | PubMed

Pogue CB, Zhou T, Nan B (2018) PlpA, a PilZ-like protein, regulates directed motility of the bacterium *Myxococcus xanthus*. *Mol Microbiol* **107**:214-228 https://doi.org/10.1111/mmi.13878 | PubMed

Popham DL, Bernhards CB (2015) Spore Peptidoglycan. *Microbiol Spectr* **3** https://doi.org/10.1128/microbiolspec.tbs-0005-2012 | PubMed

Ramirez Carbo CA, Faromiki OG, Nan B (2024) A lytic transglycosylase connects bacterial focal adhesion complexes to the peptidoglycan cell wall. *eLife* **13** https://doi.org/10.7554/elife.99273 | PubMed

Ramírez Carbó CA, Nan B (2026) Using Single-Particle Fluorescence Microscopy to Quantify Substrate Binding of Peptidoglycan-Modification Enzymes. *Bio-protocol* **16**:e5696 https://doi.org/10.21769/BioProtoc.5696 | PubMed

Rohs PDA, Bernhardt TG (2021) Growth and Division of the Peptidoglycan Matrix. *Annu Rev Microbiol* **75**:315-336 https://doi.org/10.1146/annurev-micro-020518-120056 | PubMed

Saidi F, Jolivet NY, Lemon DJ, Nakamura A, Belgrave AM, Garza AG, Veyrier FJ, Islam ST (2021) Bacterial glycocalyx integrity drives multicellular swarm biofilm dynamism. *Mol Microbiol* **116**:1151-1172 https://doi.org/10.1111/mmi.14803 | PubMed

Singh SK, SaiSree L, Amrutha RN, Reddy M (2012) Three redundant murein endopeptidases catalyse an essential cleavage step in peptidoglycan synthesis of *Escherichia coli* K12. *Mol Microbiol* **86**:1036-1051 https://doi.org/10.1111/mmi.12058 | PubMed

Sung MT, Lai YT, Huang CY, Chou LY, Shih HW, Cheng WC, Wong CH, Ma C (2009) Crystal structure of the membrane-bound bifunctional transglycosylase PBP1b from *Escherichia coli*. *Proc Natl Acad Sci U S A* **106**:8824-8829 https://doi.org/10.1073/pnas.0904030106 | PubMed

Tocheva EI, Matson EG, Morris DM, Moussavi F, Leadbetter JR, Jensen GJ (2011) Peptidoglycan remodeling and conversion of an inner membrane into an outer membrane during sporulation. *Cell* **146**:799-812 https://doi.org/10.1016/j.cell.2011.07.029 | PubMed

Tokunaga M, Imamoto N, Sakata-Sogawa K (2008) Highly inclined thin illumination enables clear single-molecule imaging in cells. *Nat Methods* **5**:159-161 https://doi.org/10.1038/nmeth1171 | PubMed

Uehara T, Parzych KR, Dinh T, Bernhardt TG (2010) Daughter cell separation is controlled by cytokinetic ring-activated cell wall hydrolysis. *EMBO J* **29**:1412-1422 https://doi.org/10.1038/emboj.2010.36 | PubMed

van Heijenoort J (2011) Peptidoglycan hydrolases of *Escherichia coli*. *Microbiol Mol Biol Rev* **75**:636-663 https://doi.org/10.1128/mmbr.00022-11 | PubMed

Voelz H, Dworkin M (1962) Fine structure of *Myxococcus xanthus* during morphogenesis. *J Bacteriol* **84**:943-952 https://doi.org/10.1128/jb.84.5.943-952.1962 | PubMed

Waite DW, Chuvochina M, Pelikan C, Parks DH, Yilmaz P, Wagner M, Loy A, Naganuma T, Nakai R, Whitman WB, *et al.* (2020) Proposal to reclassify the proteobacterial classes Deltaproteobacteria and Oligoflexia, and the phylum Thermodesulfobacteria into four phyla reflecting major functional capabilities. *Int J Syst Evol Microbiol* **70**:5972-6016 https://doi.org/10.1099/ijsem.0.004213 | PubMed

Wartel M, Ducret A, Thutupalli S, Czerwinski F, Le Gall AV, Mauriello EM, Bergam P, Brun YV, Shaevitz J, Mignot T (2013) A versatile class of cell surface directional motors gives rise to gliding motility and sporulation in *Myxococcus xanthus*. *PLoS Biol* **11**:e1001728 https://doi.org/10.1371/journal.pbio.1001728 | PubMed

Weaver A, Taguchi A, Dorr T (2023) Masters of Misdirection: Peptidoglycan Glycosidases in Bacterial Growth. *J Bacteriol* **205**:e0042822 https://doi.org/10.1128/jb.00428-22 | PubMed

Weaver AI, Alvarez L, Rosch KM, Ahmed A, Wang GS, van Nieuwenhze MS, Cava F, Dorr T (2022) Lytic transglycosylases mitigate periplasmic crowding by degrading soluble cell wall turnover products. *eLife* **11** https://doi.org/10.7554/elife.73178 | PubMed

White D, Dworkin M, Tipper DJ (1968) Peptidoglycan of *Myxococcus xanthus*: structure and relation to morphogenesis. *J Bacteriol* **95**:2186-2197 https://doi.org/10.1128/jb.95.6.2186-2197.1968 | PubMed

Williams AH, Wheeler R, Rateau L, Malosse C, Chamot-Rooke J, Haouz A, Taha MK, Boneca IG (2018) A step-by-step in crystallo guide to bond cleavage and 1,6-anhydro-sugar product synthesis by a peptidoglycan-degrading lytic transglycosylase. *J Biol Chem* **293**:6000-6010 https://doi.org/10.1074/jbc.ra117.001095 | PubMed

Yang X, McQuillen R, Lyu Z, Phillips-Mason P, De La Cruz A, McCausland JW, Liang H, DeMeester KE, Santiago CC, Grimes CL, *et al.* (2021) A two-track model for the spatiotemporal coordination of bacterial septal cell wall synthesis revealed by single-molecule imaging of FtsW. *Nat Microbiol* **6**:584-593 https://doi.org/10.1038/s41564-020-00853-0 | PubMed

Yutin N, Galperin MY (2013) A genomic update on clostridial phylogeny: Gram-negative spore formers and other misplaced clostridia. *Environ Microbiol* **15**:2631-2641 https://doi.org/10.1111/1462-2920.12173 | PubMed

Zhang H, Mulholland GA, Seef S, Zhu S, Liu J, Mignot T, Nan B (2020) Establishing rod shape from spherical, peptidoglycan-deficient bacterial spores. *Proc Natl Acad Sci U S A* **117**:14444-14452 https://doi.org/10.1073/pnas.2001384117 | PubMed

Zhang H, Venkatesan S, Nan B (2021) *Myxococcus xanthus* as a Model Organism for Peptidoglycan Assembly and Bacterial Morphogenesis. *Microorganisms* **9** https://doi.org/10.3390/microorganisms9050916 | PubMed

Zhang H, Venkatesan S, Ng E, Nan B (2023a) Coordinated peptidoglycan synthases and hydrolases stabilize the bacterial cell wall. GitHub. https://github.com/NanLabMyxo/Rod_shape_paper/tree/Rod_shape_paper

Zhang H, Venkatesan S, Ng E, Nan B (2023b) Coordinated peptidoglycan synthases and hydrolases stabilize the bacterial cell wall. *Nature communications* **14**:5357 https://doi.org/10.1038/s41467-023-41082-3 | PubMed

Peer reviews

Reviewer #2 (Public review):

The authors initial goal was to demonstrate loss of PG during the slow sporulation process of Myxococcus xanthus, with examination of the PG degradation products in order to implicate possible enzymes involved. Upon finding a predominance of LTG products, they examined sporulation in strains lacking each of the 14 candidate LTGs encoded in the genome, leading to the identification of two sporulation-linked LTGs. An extensive characterization of the roles played by these LTGs. One LTG is responsible for the slow sporulation PG degradation, while another is required for the rapid sporulation process. Interestingly, the "slow" LTG seems to provide an important regulatory brake on the rapid enzyme. Single molecule fluorescent tracking of these enzymes was used to develop a model for their interaction with PG that mimics their observed activity. The rate of PG synthesis activity was also shown to impact the rate of PG degradation, suggesting potential interplay between the synthetic and degradative enzymes.

Strengths:

The genetic analysis to identify sporulation-linked LTGs and their effects on growth sporulation, and spore properties was well done and productive. The fluorescence microscopy to track LTG mobility, presumably tied to activity, produced a convincing argument about the mechanism of regulation of one LTG by another. The authors have responded well to most points of the previous review.

Weaknesses:

While the impact of LTGs on sporulation was clearly demonstrated, the PG analysis that resulted in the study of LTGs raised some important unanswered questions. The analyses suggest that the PG is degraded to quite small fragments, which would normally be lost during the purification of PG. The conclusions concerning the PG degradation during sporulation needs to be clarified, as described below. The authors suggest a "new mechanism of sporulation" when they have actually simply identified an important factor (PG degradation by LTGs) within a complex "process of sporulation". This needs to be reflected also in title of the paper.

https://doi.org/10.7554/eLife.108250.2.sa1

Author response:

The following is the authors' response to the original reviews.

> ***Public Reviews:***
>
> ***Reviewer #1 (Public review):***
>
> *Summary:*
>
> *Ramirez Carbo et al. use the powerful M. xanthus spore morphogenesis model to address fundamental mechanisms in coordinated peptidoglycan remodeling and degradation. As peptidoglycan is an essential macromolecule and difficult to study in vivo, the authors use indirect but important methodology. The authors first identify two lytic transglycosylase (Ltg) enzymes necessary for spore morphogenesis using mutant*

phenotypic studies. They characterize these mutants for their role in coordinating spore morphogenesis induced either in fruiting bodies (starvation-dependent) or in liquid-rich media conditions (chemical-dependent). They conclude from these phenotypic and epistatic analyses that LtgA is necessary for morphogenesis during chemical-induced sporulation, and LtgB appears to be necessary to coordinate LtgA activity by interfering with LtgA function. Under starvation-induced sporulation, the absence of LtgB interferes with the building of fruiting bodies. LtgA does not appear to play a primary role in promoting aggregation into fruiting bodies, nor in degradation of peptidoglycan as assayed by loss of signal in anti-PG immunofluorescence. The authors demonstrate that the purified periplasmic domain of LtgA is highly active in degrading purified PG sacculi in vitro, while that of LtgB is highly reduced (relative to LtgA or lysozyme). The authors use photoactivated mCherry Lyt fusions and PALM to track the fusion protein mobility, which they state correlates with activity as immobilization results from PG binding. They demonstrate that in vegetative cells, a greater proportion of LtgA-PAmCh is more immobile (more active) than LtgB-PAmCh, but that directly after chemical-induction of sporulation, LtgB-PAmCh becomes more immobile (active). These analyses in the partner mutant backgrounds suggest that LtgA-PAmCh is more immobile (less active) in the absence of LtgB, but the reverse is not observed. Finally, the authors demonstrate that overexpression of LtgA in vegetative conditions leads to cell rounding, likely because of uncontrolled PG degradation, while overexpression of LtgB displays no phenotype.

Strengths:

This paper capitalizes on a novel spore morphogenesis mechanism to define proteins and mechanisms involved in peptidoglycan reorganization. The authors use the powerful PALM microscopy technique to assess Ltg activity in vivo by assaying for immobility as a proxy for PG binding. The authors elucidate a novel mechanism by which two Ltg's function together- with one (LtgB) seeming to regulate the activity of the other (the primary Ltg).

Despite some weaknesses, there is no question that this study provides important insight into mechanisms of peptidoglycan remodeling- a difficult but highly impactful area of study with implications for the development of novel therapeutics and the discovery of mechanisms of fundamental bacterial physiology.

Weaknesses:

In many places, the authors do not adequately justify interpretations of their assays, leading to some apparently unjustified conclusions. Many of these are minor and may just require citations to demonstrate that the interpretations are justified by previous studies (detailed in recommendations below), but two bigger concerns are as follows:

(1) It is not clear how the muropeptides listed in Figure 1 were assigned, and it is missing in the methods. In the sporulating conditions, the spectra look like combinations of multiple peaks, and the data, as stated, is not convincing to the non-specialist eye.

We thank the reviewer for raising this point. We've expanded the Methods section to give a fuller account of how muropeptides were identified. In particular, we now describe the chromatographic separation and the assignment process, which relies on comparison with published data, fragmentation patterns, retention times, and accurate mass values. We acknowledge that the chromatograms show several peaks; nevertheless, only those muropeptides that we could clearly identify by MS/MS analysis were annotated in Figure 1. This clarification is now made explicit in the figure legend in the revised version of the manuscript.

(2) The observation that the lytB mutant prevents appropriate aggregation into fruiting

> *bodies does not allow the interpretation that the absence of LtgB prevents PG morphogenesis in the starvation-induced sporulation pathway, per se. It is more likely that in the LtgB mutant, the morphogenesis program is not even triggered. This is because signaling proteins and regulators (specifically, C-signal accumulation/activated FruA), which are dependent on increased cell-cell signaling in the fruiting body, do not accumulate appropriately in shallow aggregates. C-signal/FruA are necessary to trigger the sporulation program in FBs. BTW: A hypothesis to explain the indirect effect of ltgB absence on aggregation could be that UDP-precursors are not regulated appropriately (unregulated LtyA (LtgA [sic])??), so polysaccharides necessary for motility are not properly produced.*
>
> *Along these lines, fruiting body formation does not equal sporulation, and even "darkened" fruiting bodies can be misleading, as some mutants form polysaccharideriche fruiting bodies (that appear dark under certain light conditions in the stereomicroscope) but do not sporulate efficiently. The wording in the text suggests that the authors assume that sporulation levels are normal because fruiting bodies are produced (see specific comments for details).*

We deeply appreciate this question. Seeking the answer, we repeated the fruiting body assay and found that both the *ΔltgA* and *ΔltgB* mutants formed dark aggregates that were comparable to wild-type fruiting bodies. However, these “fruiting body-like” aggregates did not contain sonication-resistant spores. Thus, regardless of the signals, either glycerol or starvation, sporulation requires both LtgA and LtgB. We have corrected the mistakes in the first submission.

> *(3) The authors repeatedly state that production of spore coat polysaccharides likely affects the PG IP staining (see below), but this is not well justified. A citation is needed if this has already been directly shown, or the language needs to be softened.*

We agree with the reviewer. We have softened our language as “However, we cannot exclude the possibility that the polysaccharide spore coats (Voelz & Dworkin, 1962) hinder antibody access to PG.”

> *(4) Better justification for the immobility of Ltg proteins in vivo as an assay for activity may be required. If this is well known in the field, it should be explicitly stated. The authors address this better in the discussion - but still state it is a correlation.*

We elaborated the justification, “Thus, when diffusive enzymes bind to PG, their mobility decreases (Lee et al., 2016; Zhang et al., 2023). For instance, DacB, another PG hydrolase, reduces its single-particle mobility in the conditions where its activity is activated (Zhang et al., 2023). By tracking single fluorescently-labeled enzyme particles, we can approximate their PG-binding in different physiological conditions and genetic backgrounds (Ramirez Carbo et al., 2024, Zhang et al., 2023, Ramírez Carbó & Nan, 2026).”

We further discussed the correlation in discussion, “The simultaneous occurrence of reduced LtgA mobility and PG degradation during glycerol-induced sporulation indicates that the molecular dynamics of LtgA accurately mirrors its enzymatic activity. Such correlation between decreased particle mobility and increased enzymatic activity applies to many other PG-related enzymes, including multiple PG polymerases in *E. coli* and the endopeptidase DacB in *M. xanthus* (Lee et al., 2016, Zhang et al., 2023, Yang et al., 2021).”

> ***Reviewer #2 (Public review):***
>
> *Summary:*
>
> *The authors' initial goal was to demonstrate loss of PG during the slow sporulation process of Myxococcus xanthus, with examination of the PG degradation products in*

> *order to implicate possible enzymes involved. Upon finding a predominance of LGT products, they examined sporulation in strains lacking each of the 14 candidate LTGs encoded in the genome, leading to the identification of two sporulation-linked LTGs. An extensive characterization of the roles played by these LTGs. One LTG is responsible for the slow sporulation PG degradation, while another is required for the rapid sporulation process. Interestingly, the "slow" LTG seems to provide an important regulatory brake on the rapid enzyme. Single-molecule fluorescent tracking of these enzymes was used to develop a model for their interaction with PG that mimics their observed activity. The rate of PG synthesis activity was also shown to impact the rate of PG degradation, suggesting potential interplay between the synthetic and degradative enzymes.*
>
> *Strengths:*
>
> *The genetic analysis to identify sporulation-linked LTGs and their effects on growth, sporulation, and spore properties was well done and productive. The fluorescence microscopy to track LTG mobility, presumably tied to activity, produced a convincing argument about the mechanism of regulation of one LTG by another.*
>
> *Weaknesses:*
>
> *While the impact of LTGs on sporulation was clearly demonstrated, the PG analysis that resulted from the study of LTGs raised some important unanswered questions. The analyses suggest that the PG is degraded to quite small fragments, which would normally be lost during the purification of PG. How these small fragments were thus detected is unclear, and this suggests a more complex story concerning PG metabolism during sporulation. An anti-PG antibody is used to quantify PG in the spores, but it is not made clear what the specificity of this antibody is, and thus whether it would recognize the LTG -altered PG of the spore. The authors suggest a "new mechanism of sporulation" when they have actually simply identified an important factor (PG degradation by LTGs) within a complex "process of sporulation".*
>
> ***Recommendations for the authors:***
>
> ***Reviewer #1 (Recommendations for the authors):***
>
> *Details on places in the text that could be improved:*
>
> *(1) Line 77: more appropriate "homologs of the sporulation genes"*

Corrected.

> *(2) Line 137-139. Where are the 14 KO mutant data? Only showing the ones with phenotypes? Needs a citation if published elsewhere.*

The phenotypes of other mutants are shown in the new Fig. S1.

> *(3) Line 144 and later: why "ORF"? Are they not homologous to Ltg's??. Also, the orf designation is not in the figure, so it is hard to follow the data the authors are presenting.*

Following the reviewer's recommendation, we deleted "ORF" and presented the ORF designation in the figure legend.

> *(4) Figure 2B - add the y-axis legend to the figure (also S1B).*

Added

> *(5) Line 156: What does "same below" mean?*

Deleted “same below”.

(6) Line 161: emtA is not indicated on Figure 2D - can you reword or add to the legend??

Changed to “MltE, an LTG encoded by *Escherichia coli* emtA”

> *(7) Line 163: "opposite roles" could be a bit better defined... do you mean ltgA induces rounding and ltgB delays rounding???*

We agree with the reviewer. “opposite” was replaced by “different”.

> *(8) Line 172: But did the ltgA mutant make the same number of viable spores (not just FBs)? Can't conclude "the slow sporulation pathway only requires ltgB" if ltgA mutant was not tested.*

We agree with the reviewer. In the revised manuscript, we quantified the starvation-induced spores and found that both LtgA and LtgB are required for forming mature spores. The data are shown in Figure 3 and supplement figures.

> *(9) Line 202: might be appropriate to indicate the degree of homology (% identity over protein length).*

Added.

> *(10) Line 178, 181, and thereafter: DIC microscopy.*

Corrected.

> *(11) Line 182/183 and 190: What is the basis for the conclusion that "polysaccharides sustained unflattened structures"??*

We changed the description to “likely due to the deposition of spore coat polysaccharides that sustained unflattened cell structures (Wartel et al., 2013; Holkenbrink et al., 2014).”

> *(12) Line 185/186: What is the basis for the conclusion that ltgB only contained a small amount of PG? If it is based on reduced intensity, it is not obvious from the images presented. Quantitative analysis would better support this statement.*

We changed the description to “Sacculi from the *ΔltgB* pseudospores still contained PG but showed lower fluorescence intensity”. We also updated the figure to show the typical fluorescence intensities.

> *(13) Figure legend 3 line 245/6: It is not totally clear what the difference is, in that the white arrows are pointing to in ltgA vs ltgB mutant. Is it the proportion of large spherical objects in ltgB? What is the significance of the puncta in A vs. B?*

We updated the description in the text as “While the remaining PG sacculi of these pseudospores were largely spherical, they lost integrity during purification, with many sacculi displaying irregular shapes in the fluorescence channel (Figure 4A).” In the figure legend, we changed the description to White arrows point to the sacculi in irregular shapes.”

> *(14) Line 190-192. Again, not really seeing what the authors are identifying to conclude "irregular shapes and ruptures" could authors pin-point more specifically and quantify such structures?*

We updated the description in the text as “While the remaining PG sacculi of these pseudospores were largely spherical, they lost integrity during purification, with many sacculi displaying irregular shapes in the fluorescence channel (Figure 4A).”

> *(15) Line 194: if the authors want to make such a strong conclusion, they really should demonstrate this. Anti-spore coat antibodies are available in the field. Or take out these statements.*

We took this statement out.

> *(16) Line 210: either they lack PG, OR the antibody can't gain access? How to conclude both? Might be more accurate to say "although we can't rule out that the polysaccharide spore coat prevents access to PG"*

Following the reviewer's recommendation, we changed the description to "These fruiting body spores lacked PG-specific fluorescence (Fig. 3A), consistent with their markedly reduced PG content (Fig. 1). However, we cannot exclude the possibility that the polysaccharide spore coats (Voelz & Dworkin, 1962) hinder antibody access to PG.

> *(17) Line 217-19: This is often stated in the literature, but full glycerol-induced spore maturation requires much more than 2 hours (note the authors are using O/N glycerol induction in Figure 1). And the long starvation-induced sporulation process is likely due to the differential start of sporulation, because the cells don't all enter the aggregate at the same time.... so they are not triggered to induce sporulation at the same time.*

We agree with the reviewer on the first statement and changed "two hours" to "four hours". For the second statement, we do not completely agree. Much research showed that spore development in fruiting bodies is well synchronized, for example, in (Dworkin & Voelz, 1962), starvation-induced spores did not at 48 h.

> *(18) Line 222: What is the evidence that it is really variation in production from the van promoter? Could it also just be due to differences in the cell cycle in the population? The authors may be correct, but should be less definitive about those conclusions since they haven't measured LtgA levels directly.*

We agree with the reviewer. We changed the description to, "Upon induction with 200 μM vanillate, cells exhibited heterogeneous morphology, likely resulting from variations in LtgA expression or differences in cell cycle stages within the population." Following this suggestion, we also changed the description on murA overexpression, "Similar to the cells that overexpressed LtgA (Fig. 3B), this heterogeneity likely reflects variable *murA* induction or the unsynchronized growth stages within the population."

> *(19) Line 224: Where is the over-expressed LtgA data in Figure 2A? Is it that the authors are referring to over-expressed murA data, and the point is that overexpression of this kind of gene can lead to veg cell rounding? If the latter, this should be specifically stated in the text.*

We apologize for this mistake. The data were shown in Fig. 3B, rather than Fig. 2A, 3B.

> *(20) Line 224: Did the authors test that LtgB is stably overproduced in veg cells? It could be that LtgB is turned over while LtgA is not. From the purified protein blot in Figure 3C, it does look like LtgB contains a degradation product (which is perhaps inhibiting the LtgB activity).*
>
> *(21) Line 229: AgmT? Do the authors mean Ltg?*

Corrected.

> *(22) Line 238: Is "rate" the right word? Technically, kinetics haven't been measured. Could state "LtgB less active" or "less efficient"?*

Changed.

> *(23) Line 255: "ltgB shows a slight increase in expression during slow sporulation". Do the authors mean over the entire dev time course or specifically during the sporulation phase (which will be different timing for DZ2 vs DK1622)?*

We clarified the description as “Consistent with its role in PG degradation, in a microarray-based transcriptome analysis, *ltgA* transcription was found to increase about twofold during rapid sporulation (4 h) but remain unchanged during slow sporulation (96 h). in the closely related DK1622 strain (Muller et al., 2010). Conversely, *ltgB* expression gradually rises during slow sporulation, reaching 1.8 times the vegetative level at 96 h, while remaining stable during rapid sporulation (Muller et al., 2010, Munoz-Dorado et al., 2019).”

> *(24) Line 278: This needs to be corrected. The authors have shown that production of fruiting bodies is not affected by the fusions. (also in Fig. S1 legend). This is really not the same as sporulation efficiency.*

We changed the description to “the PAmCherry tags did not affect the formation of either glycerol-induced spores or starvation-induced fruiting bodies”.

> *(25) Figure S1A: panel A: Is there a deg product partially cut off at the bottom of the gel? (or is this a non-specific cross-reactive band). What is the predicted molecular mass for both proteins with the PAmCherry fusion? What conditions were these lysates generated from: veg prior to glycerol induction? I understand there are probably no antibodies available to LtgA or B, but it is important to note that it is not possible to know if there is simultaneously wt LtgA or B produced (by cleavage and degradation of the mCh fusion). Panel B: Were the differences in l/w between wt and the fusion strains tested to see if there really were no significant differences? Please state in the text (it looks like the data variance is higher in the fusion strains relative to the wt at 1 hr).*

The bands at the bottom of the gel are the running front that appear in both lanes. They are not mCherry because there estimated molecular weight is much lower than that of mCherry (26.3 kDa). To avoid confusion, we cut these bands from the figure. The expression of both fusion proteins was detected from vegetative cells, which was clarified in the legend. The predicted molecular weights of them were provided in the legend too.

> *(26) Figure S1C: The ability to make fb is not the same as the production of spores. The authors should test the number of viable spores produced under starvation conditions, if they want to state starvation-induced sporulation is not affected by the fusions.*

We agree with the reviewer. We quantified starvation-induced sporulation in the revised manuscript.

> *(27) Line 399: Figure S2 looks at fb formation in the absence of vanillate, not sporulation.*

We changed the description to “cells grown without vanillate progressed normally through glycerol-induced sporulation and starvation-induced fruiting body formation”.

We also quantified starvation-induced sporulation in the revised manuscript.

> *(28) Line 281: How many fold is the ltgA transcript reduced compared to the ltgB? (i.e., If it is 1.2 fold reduced that may not be as worth mentioning as if it was 5-10 fold reduced).*

ltgA transcription in vegetative cells was detected in a microarray (Muller et al., 2010) but not reported in RNAseq (Munoz-Dorado et al., 2019), significantly different from that of *ltgB*. We pointed this out in the revised manuscript.

> *(29) Figure 4B legend line 358. Define D (should it be italicized?).*

Corrected.

> *(30) Line 363: Please define how significance was calculated. Is this the p-value?*

We deleted the word “significant”.

> *(31) Line 298: How do the authors know immobility is from binding to PG? Provide a reference if this is well-known.*

The rationale and references have been mentioned at the beginning of this section.

> *(32) Line 302 and thereafter: suggest "2.62 × 10-2 (plus minus) 2.0 × 10-3 μm2/s" is presented as "2.62 (plus minus) 0.20 × 10-2 μm2/s" for easier reading; switch to past tense (Were not are).*

Changed following the reviewer’s recommendation.

> *(33) Line 310: "suggest" not "indicate", because binding of PG was directly tested.*

Corrected.

> *(34) Line 341: "confirming it restricts access" seems very strong wording. Suggest: may compete with.*

Changed.

> *(35) Line 392: SOME fb are larger- many are significantly smaller.*

Because fruiting body sizes do not reflect sporulation efficiency, we removed this description.

> *(36) Figure S2 legend. Leaky expression; or on fruiting body formation.*

Corrected.

> *(37) Line 436: stationary phase cells decrease PG synthesis- does this increase PG degradation? Perhaps it does lead to the death phase, which is striking in M. xanthus....*

How do cells die, either through death phase or under antibiotic stresses, is not well understood (Baquero & Levin, 2021) Very likely, cell death is due to the accumulation of oxidative damages (Kohanski et al., 2007) and cell lysis could be a byproduct of cell death, when cells lose control of the enzymes that break PG. While cell death is a great topic to investigate, it is beyond the scope of this study.

> *(38) Line 507: washed.*

Corrected.

> *(39) Line 524 (514 [sic]) and thereafter: sacculi.*

Corrected.

> *(40) Line 587: reference for cell lysis procedure?*

The procedures of cell lysis, column loading and elusion were described in details “...cells were harvested by centrifugation at 6,000 × g for 20 min and lysed by sonication in buffer A (20 mM Tris-HCl pH 8.0, 200 mM NaCl), (Nan et al., 2010, Nan et al., 2006). Proteins were loaded to an NGC™ Chromatography System (BIO-RAD) and 5-ml HisTrap™ columns (Cytiva)

and eluted by buffer B (20 mM Tris-HCl pH 8.0, 200 mM NaCl, 500 mM immidazole) (Pogue et al., 2018, Nan et al., 2010)."

> *(41) Line 269: by microscopy (or "under THE microscope").*

Corrected.

> *(42) Line 271: THE cell/PG.*

"The" added.

> *(43) Line 603: OR not and.*

Corrected.

> *(44) Line 497 (and elsewhere): Is it really CFU? If determined by OD, then not technically CFU because some cells will not grow into colonies.*

We agree with the reviewer. Cell concentrations were determined by OD. "CFU" was deleted.

> *(45) Line 506: washed.*

Same as recommendation (38). Corrected.

> *(46) Line 521: min.*

Corrected.

> *(47) Line 532: How were peaks assigned?*

We described peak assignment in details in the revised manuscript, "Muropeptides were assigned based on: (i) accurate mass matching to theoretical monoisotopic masses of expected *M. xanthus* PG building blocks (Bui et al., 2009, White et al., 1968) and (ii) comparison of retention times with those reported in previous analysis with similar PG compositions."

> ***Reviewer #2 (Recommendations for the authors):***
>
> *(1) If almost all the muropeptides detected in spores are anhydro products of LTGs, then it might be expected that these are all very small peptidoglycan fragments in the spores. If the anhydro units were at the ends of short PG chains, then muramidase digestion would release similar amounts of non-anhydro products, but none are detected. So, is muramidase digestion doing anything to the PG derived from the spores? Is muramidase digestion required to observe the spore muropeptide pattern? A control sample in which muramidase digestion is omitted would answer these questions.*

Muramidase digestion is essential for solubilizing PG into different muropeptides for UPLC analysis. In each sample, both anhydro and non-anhydro products were detected. In our original submission, we pointed out that "The two spore types showed similar profiles of a discernible presence of muropeptides that resembled those found in vegetative cells, albeit in significantly reduced quantities (Fig. 1)." We clarified the PG analysis. "The purification procedure yields only sedimentable PG, as all soluble fragments are removed during the washing steps. The resulting sacculi were then digested with muramidase, and the solubilized muropeptides were analyzed by UPLC (see Materials and Methods). The chromatograms in Fig. 1 reflect the muropeptides released specifically from the sedimented sacculus fraction." Because muramidase release polysaccharides or disaccharides, so it's digestion does not release nonanhydro GlcNAc species, which is why we did not see equal amounts of anhydro and non-anhydro products. In our case, over 90% of the polysaccharides and disaccharides contain Anhydro-MurNAc. The dominance of anhydro products indicates that LTGs cut very frequently on glycan chains.

> *(2) This also raises the question of how these very small peptidoglycan fragments are even retained in the spores. They would be expected to be lost during spore purification or during PG purification prior to muramidase digestion. How do you even purify sacculi when the spores have no PG chains? One could theorize that the polysaccharide coats hold everything in, but then the PG would be protected from muramidase digestion.*

We thank the reviewer for this question. Our analysis suggests that *M. xanthus* spores do not lack PG entirely but retain a residual PG mesh that is still crosslinked. Such crosslinked material sediments during PG purification and remains accessible to muramidase, which hydrolyses internal glycosidic bonds and releases anhydro muropeptides. Non-crosslinked fragments would indeed be washed away during purification steps, so the detected muropeptides reflect the structure of this residual sacculus (Fig. 1).

> *(3) What is the anti-PG antibody recognizing, the glycan backbone, the peptide side chain, or both? Can the antibody recognize the very short anhydro-containing disaccharides proposed to be predominant in spores? If not, then the PG quantification using the antibody is not accurate.*

The structures recognized by the anti-PG antibodies are unknown. Our samples do not contain small degradation products, which was clarified in the revised manuscript, “To answer this question, we purified cell sacculi and used immunofluorescence and an anti-PG serum (de Pedro et al., 1997) to visualize the remaining PG.” We used immunofluorescence to display the PG scaffolds remained in each sample and we did not perform any quantitative analysis based on the images.

> *(4) Lines 325-327: This is a speculative conclusion and should be stated as such, i.e., "may control the pace.." This conclusion could be somewhat more strongly stated at the end of the next section, around lines 345-350.*

Moved following the reviewer’s recommendation.

> *(5) Lines 403-404: This first sentence of the discussion seems completely dissociated from the topic of the paper; it should be deleted.*

Deleted.

> *(6) Lines 404-405. I am not convinced that these findings "elucidate a new mechanism of sporulation." The study was undertaken because PG degradation was already tied to sporulation in a previous study. Furthermore, I am not sure that PG degradation is a "mechanism of sporulation." It is clearly an important step in sporulation of this species, but is it the driving "mechanism"?*

We tuned down our statement as “Our findings demonstrate that *M. xanthus*, a nonfirmicute bacterium, relies on PG degradation to change cell shape during sporulation”.

> *(7) Lines 510-516 describe PG purification from vegetative cells. How was this process modified for spores?*

We apologize for the confusion. The process was clarified as “For PG analysis, samples were processed as previously described for Gram-negative bacteria (Alvarez et al., 2016; Desmarais et al., 2013). Vegetative cells were harvested at mid-stationary phase by centrifugation (30 min, 8,000 g). Vegetative cells and purified spores (as described in the previous section) were resuspended…”.

Alvarez, L., Hernandez, S.B., de Pedro, M.A., and Cava, F. (2016) Ultra-Sensitive, High-Resolution Liquid Chromatography Methods for the High-Throughput Quantitative Analysis of Bacterial Cell Wall Chemistry and Structure. Methods Mol Biol 1440: 1127.

Baquero, F., and Levin, B.R. (2021) Proximate and ultimate causes of the bactericidal action of antibiotics. Nat Rev Microbiol 19: 123-132.

Bui, N.K., Gray, J., Schwarz, H., Schumann, P., Blanot, D., and Vollmer, W. (2009) The peptidoglycan sacculus of Myxococcus xanthus has unusual structural features and is degraded during glycerol-induced myxospore development. J Bacteriol 191: 494505.

de Pedro, M.A., Quintela, J.C., Holtje, J.V., and Schwarz, H. (1997) Murein segregation in Escherichia coli. J Bacteriol 179: 2823-2834.

Desmarais, S.M., De Pedro, M.A., Cava, F., and Huang, K.C. (2013) Peptidoglycan at its peaks: how chromatographic analyses can reveal bacterial cell wall structure and assembly. Mol Microbiol 89: 1-13.

Dworkin, M., and Voelz, H. (1962) The formation and germination of microcysts in Myxococcus xanthus. J Gen Microbiol 28: 81-85.

Holkenbrink, C., Hoiczyk, E., Kahnt, J., and Higgs, P.I. (2014) Synthesis and assembly of a novel glycan layer in Myxococcus xanthus spores. J Biol Chem 289: 32364-32378.

Kohanski, M.A., Dwyer, D.J., Hayete, B., Lawrence, C.A., and Collins, J.J. (2007) A common mechanism of cellular death induced by bactericidal antibiotics. Cell 130: 797-810.

Lee, T.K., Meng, K., Shi, H., and Huang, K.C. (2016) Single-molecule imaging reveals modulation of cell wall synthesis dynamics in live bacterial cells. Nature communications 7: 13170.

Muller, F.D., Treuner-Lange, A., Heider, J., Huntley, S.M., and Higgs, P.I. (2010) Global transcriptome analysis of spore formation in Myxococcus xanthus reveals a locus necessary for cell diberentiation. BMC Genomics 11: 264.

Munoz-Dorado, J., Moraleda-Munoz, A., Marcos-Torres, F.J., Contreras-Moreno, F.J., MartinCuadrado, A.B., Schrader, J.M., Higgs, P.I., and Perez, J. (2019) Transcriptome dynamics of the Myxococcus xanthus multicellular developmental program. Elife 8.

Nan, B., Liu, X., Zhou, Y., Liu, J., Zhang, L., Wen, J., Zhang, X., Su, X.D., and Wang, Y.P. (2010) From signal perception to signal transduction: ligand-induced dimeric switch of DctB sensory domain in solution. Mol Microbiol 75: 1484-1494.

Nan, B., Zhou, Y., Liang, Y.H., Wen, J., Ma, Q., Zhang, S., Wang, Y., and Su, X.D. (2006) Purification and preliminary X-ray crystallographic analysis of the ligand-binding domain of Sinorhizobium meliloti DctB. Biochim Biophys Acta 1764: 839-841.

Pogue, C.B., Zhou, T., and Nan, B. (2018) PlpA, a PilZ-like protein, regulates directed motility of the bacterium Myxococcus xanthus. Mol Microbiol 107: 214-228.

Ramirez Carbo, C.A., Faromiki, O.G., and Nan, B. (2024) A lytic transglycosylase connects bacterial focal adhesion complexes to the peptidoglycan cell wall. Elife 13.

Ramírez Carbó, C.A., and Nan, B. (2026) Using Single-Particle Fluorescence Microscopy to Quantify Substrate Binding of Peptidoglycan-Modification Enzymes. Bio-protocol 16: e5696.

Voelz, H., and Dworkin, M. (1962) Fine structure of Myxococcus xanthus during morphogenesis. J Bacteriol 84: 943-952.

Wartel, M., Ducret, A., Thutupalli, S., Czerwinski, F., Le Gall, A.V., Mauriello, E.M., Bergam, P., Brun, Y.V., Shaevitz, J., and Mignot, T. (2013) A versatile class of cell surface directional motors gives rise to gliding motility and sporulation in Myxococcus xanthus. PLoS Biol 11: e1001728.

White, D., Dworkin, M., and Tipper, D.J. (1968) Peptidoglycan of Myxococcus xanthus: structure and relation to morphogenesis. J Bacteriol 95: 2186-2197.

Yang, X., McQuillen, R., Lyu, Z., Phillips-Mason, P., De La Cruz, A., McCausland, J.W., Liang, H., DeMeester, K.E., Santiago, C.C., Grimes, C.L., de Boer, P., and Xiao, J. (2021) A two-track model for the spatiotemporal coordination of bacterial septal cell wall synthesis revealed by single-molecule imaging of FtsW. Nat Microbiol 6: 584-593.

Zhang, H., Venkatesan, S., Ng, E., and Nan, B. (2023) Coordinated peptidoglycan synthases and hydrolases stabilize the bacterial cell wall. Nature communications 14: 5357.

https://doi.org/10.7554/eLife.108250.2.sa0